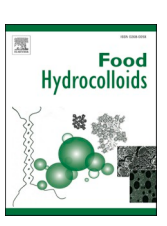
ELSEVIER

Contents lists available at ScienceDirect

Food Hydrocolloids

journal homepage: www.elsevier.com/locate/foodhyd



Chlorella vulgaris protein isolate effectively protects Lacticaseibacillus rhamnosus GG viability during processing, storage, and in vitro digestion

Jennyfer Fortuin ^{a,b}, Céline C. Leclercq ^a, Rayssa K. Silva ^c, Alexander S. Shaplov ^a, Servane Contal ^a, Sébastien Cambier ^a, Marcus Iken ^d, Vincenzo Fogliano ^b, Christos Soukoulis ^{a,*}

- ^a Luxembourg Institute of Science and Technology (LIST), 5 Avenue des Hauts Fourneaux, L4362, Esch-sur-Alzette, Luxembourg
- ^b Food Quality and Design Group (FQD), Wageningen University and Research (WUR), 6708 NL, Wageningen, the Netherlands
- ^c Laboratory of Microbial Genetics, Department of Genetics, Federal University of Pernambuco, Recife, PE, Brazil
- ^d PM International AG, Schengen, Luxembourg

ARTICLE INFO

Keywords: Microalgae Protein isolate Probiotics Encapsulation Viability In vitro digestion

ABSTRACT

This study examined the protective effect of *Chlorella vulgaris* protein isolate (CPI) on the biological activity of *Lacticaseibacillus rhamnosus* GG (LGG) during lyophilisation, storage, and *in vitro* digestion. Prior to lyophilisation, the probiotic suspensions were either fermented to pH 4.5 (CF) or left untreated (CNT). The microstructure, physicochemical, and thermal properties of the resulting probiotic powders were analysed, along with the LGG cell adhesion to an *in vitro* intestinal epithelium co-culture (Caco-2/HT29-MTX) model. The powders exhibited a compact, flaky, microporous structure with sharp edges. No significant effect of fermentation on the thermal properties of the powders was detected. A hybrid type II–III water vapour sorption isotherm was observed for all samples. The protein secondary structure of the samples consisted mainly of α -helix (68–75 %), followed by β -sheet (20–27 %) and aggregated strands (3–5 %). Embedment of LGG cells in CPI-based matrices provided effective lyoprotection, with CNT offering greater stability than CF. Elevated storage temperature and relative humidity (RH) conditions accelerated LGG inactivation, particularly in CF. While a sufficient proportion of LGG cells survived the harsh conditions of *in vitro* digestion, pre-fermentation had a negligible impact. Additionally, the adhesion capacity of the LGG cells to the intestinal mucus layer was satisfactory (>4 log CFU g⁻¹). Overall, CPI exhibits strong stabilising properties for LGG viability and represents a promising single-cell-based alternative to conventional (dairy or plant) proteins for probiotic food formulations.

1. Introduction

Probiotics play a central role in maintaining gut health and homeostasis while also contributing to the health of the reproductive tract, oral cavity, lungs, skin, and gut-brain axis (Mafe et al., 2025; Qadri et al., 2024). These beneficial microorganisms, such as yeast, *Bifidobacteria* or *Lactobacilli*, naturally occur in various fermented foods like yoghurt, cheese, kefir, sauerkraut and kimchi (Maftei et al., 2024). However, processed foods and nutraceuticals fortified with probiotics offer an alternative way of orally delivering enough (>6 log CFU g⁻¹) living probiotic cells (Kiepś & Dembczyński, 2022). Encapsulation — a physicochemical process of embedding labile bioactives, including living microorganisms, within engineered micro- or nano-structures — is a

widely adopted approach to preserve the biological activity of probiotics (Bhutto et al., 2025; de Deus et al., 2024; Gu et al., 2022; Kiepś & Dembczyński, 2022; Yao et al., 2020). An effective encapsulation system must provide sufficient protection against various external stressors encountered during processing and storage, such as temperature fluctuations, pH changes, as well as exposure to moisture, oxygen, osmotic stress, and mechanical damage (Capozzi et al., 2016; Gu et al., 2022; Yao et al., 2020). Additionally, it should support minimal cell damage during gastrointestinal passage, ensure sustained matrix breakdown and targeted probiotic release, and promote adhesion to gut mucosa (Dos Santos Morais et al., 2022; Garcia-Brand et al., 2022; Gu et al., 2022; Seifert et al., 2019).

Dehydration techniques like lyophilisation and spray drying are

This article is part of a special issue entitled: 22nd Gums and Stabilisers published in Food Hydrocolloids.

E-mail address: christos.soukoulis@list.lu (C. Soukoulis).

^{*} Corresponding author.

widely used to produce dry carriers for living cells (Aschenbrenner et al., 2015; Burgain et al., 2015). These carriers typically combine thermoplastic biopolymers (e.g., starch, gums or proteins) with lyo- or thermo-protective substances such as sugars, polyols, or maltodextrins (Broeckx et al., 2017; Schwab et al., 2007). Prebiotics, like fructo-, galacto- or xylo-oligosaccharides, can enhance cell growth and resilience under stress (Capela et al., 2006). Milk proteins, such as whey or caseins, are often used for their ability to stabilise probiotics by supporting cell adhesion and protecting membrane integrity via non-covalent and electrostatic interactions (Gomand et al., 2019; Soukoulis, Behboudi-Jobbehdar et al., 2014; Soukoulis, Yonekura, et al., 2014). However, their use poses issues related to allergenicity, sustainability, and dietary restrictions (Henchion et al., 2017). To address these issues and align with the growing demand for sustainable and healthy dietary proteins, incorporating microalgal protein in food and nutraceutical product development presents promising innovation opportunities. In a recent study (Fortuin et al., 2024), we have shown that proteins obtained from Arthrospira platensis (spirulina) offered a satisfactory protection of LGG cells in comparison to whey protein isolate (WPI). Therefore, single-cell sourced proteins may offer an excellent alternative to dairy proteins for the development of probiotic food supplements.

Microalgae are unicellular, oxygen-producing, photosynthetic microorganisms found in aquatic environments (Grossmann et al., 2020). Chlorella vulgaris, a well-studied microalgal species commonly known as chlorella, is widely cultivated, rich in proteins (up to 67 % of its dry weight) and pigments (chlorophyll a and b, and carotenoids), as well as minerals and vitamins (Safi et al., 2014). In addition, chlorella proteins are of high biological value due to their well-balanced essential amino acid profile and high digestibility (up to 85 %) (Becker, 2007; Bito et al., 2020; Safi, Charton, Pignolet, Pontalier, & Vaca-Garcia, 2013). Proteins obtained from chlorella exhibit excellent emulsifying, acid- and heat-induced gelation properties (Chen et al., 2024; Grossmann et al., 2019). The molecular weight of chlorella proteins ranges from 12 to 120 kDa, while the majority of the proteins have a molecular weight between 39 and 75 kDa (Safi et al., 2014). Additionally, the use of Chlorella sp. biomass or its bioactive fractions in dietary food supplements is known to confer several health benefits, i.e., improvement of digestive disorders, defence against pathogenic infections, reduced intestinal translocation of bacteria and endotoxin or inhibition of cancer cell growth (Huang et al., 2024).

Recent studies have highlighted the protective effects of *Chlorella* sp. on the viability of *Lactobacilli* and *Bifidobacteria* (Beheshtipour et al., 2012; Cantú-Bernal et al., 2020; Meireles Mafaldo et al., 2022). In these studies, chlorella biomass was either incorporated into fermented semi-solid dairy products or lyophilised probiotic powders. For example, the addition of *Chlorella sorokiniana* into flan enhanced the survival of *L. plantarum* and *B. longum* during storage under chilled conditions (4 °C) (Cantú-Bernal et al., 2020). Similarly, a significant increase in the viability of *L. acidophilus* and *B. lactis* was observed when at least 0.5 % *Chlorella vulgaris* was incorporated into yoghurt (Beheshtipour et al., 2012). Furthermore, the use of intact biomass of *Chlorella vulgaris* conferred promising protective cell-stabilising effects on *L. acidophilus* and *L. casei* during lyophilisation, refrigerated storage (4 °C) and simulated *in vitro* digestion (Meireles Mafaldo et al., 2022).

Heretofore, research has primarily focused on incorporating minimally processed chlorella biomass into dairy-based probiotic formulations or using it as a protective matrix for probiotics. However, the effect of CPI on the viability of LGG cells embedded in carbohydrate-based dry particulates containing bulking agents (maltodextrin) and cryoprotectants (trehalose and glucose) remains unexplored. In this context, it is hypothesized that the physicochemical, thermal and structure conformational properties of CPI are inextricably associated with its LGG cell stabilising potential during processing (lyophilisation), storage, and *in vitro* digestion, as well as its gut adhesion promoting properties. To assess the impact of the lyophilisate precursor microstructure and the

adaptation of LGG to acidic conditions, precursor solutions were either left untreated (CNT) or fermented (CF) with LGG to a pH of 4.5 prior to lyophilisation. The probiotic powders were analysed for their physicochemical, microstructural, and thermal properties. The impact of CPI on LGG viability during lyophilisation, accelerated storage, and *in vitro* digestion was assessed, along with its potential to enhance LGG adhesion in a gut epithelium co-culture model (Caco-2/HT29-MTX). Finally, the proteomic, peptidomic and free amino acids profile of the gastric and intestinal digesta were determined.

2. Materials and methods

2.1. Materials

Chlorella dry biomass, D-glucose, trehalose and maltodextrin (Maltosweet 150, 15 DE, Tate & Lyle S.A.) were purchased from Sevenhills Wholefoods (Sheffield, United Kingdom), Sigma-Aldrich (Leuven, Belgium), Louis-François (Croissy-Beaubourg, France) and Elton SA (Athens, Greece), respectively. De Man, Rogosa, and Sharpe (MRS) precast plates and MRS culture media were purchased from Thermo Scientific Oxoid (Merelbeke, Belgium) and Carl Roth (Karlsruhe, Germany), respectively. LGG ATCC 53103 was procured from VTT Technical Research Centre of Finland Ltd (Espoo, Finland). All other chemicals were of analytical grade and were purchased from Sigma-Aldrich (Leuven, Belgium).

2.2. Methods

2.2.1. Isolation of chlorella proteins

Chlorella biomass solids (10 % wt.) were dispersed into MilliQ water (18.2 m Ω , Millipore Inc., United States) and hydrated overnight under gentle stirring without pH adjustment (pH_{biomass} \approx 6.5). For the separation of the soluble and insoluble biomass, the suspension was centrifuged twice (Multifuge X3R, Fiberlite F14-6, ThermoFisher, Belgium, 18.566 g, 15 min, 4 °C). In order to precipitate the proteins present in the supernatant at the isoelectric point (Chen et al., 2024; Ursu et al., 2014), the pH was adjusted to pH 4 using 1 M HCl. The pH was adjusted every 15 min and kept at pH 4 for 1 h in total. To collect the precipitated proteins, the suspension was centrifuged (18.566 g, 15 min, 4 $^{\circ}$ C), the pellet was washed with MilliQ and centrifuged again (18.566 g, 15 min, 4 °C). The collected protein rich pellet was dispersed into MilliQ and the pH was adjusted to pH 7 with 1 M NaOH. The suspension was stirred, and the pH was adjusted to pH 7 until complete solubilisation of the aggregates. Afterwards, the suspension was dialysed (SpectraPor 4 Dialysis Membrane, Standard RC Tubing, width flat: 75 mm, Ø 48 mm, 12 kDa cut-off) against MilliQ for 48 h in order to remove the salts present in the dispersion. The MilliQ water was replaced every morning and evening. The dialysed chlorella dispersion was frozen at -80 °C and freeze-dried (Alpha 1-2LD Plus, Christ, Germany). The final protein isolates were stored in a desiccator (RH ~10 %, saturated LiCl solution) at room temperature.

2.2.2. Proximate composition of the protein isolate

Ash and moisture were gravimetrically determined according to the AOAC standard method. The sulfuric-acid-UV method was used to determine the carbohydrate content (Albalasmeh et al., 2013). A glucose standard curve with concentrations ranging from 0.01 to 1 mg mL⁻¹ was used for the quantification of the carbohydrate content. An elemental analyser (Elementar Vario Cube, Langensenbold, Germany) was used for the determination of the protein content. The protein content was determined based on the DUMAS method (nitrogen-to-protein conversion factor: 5.96 (Safi, Charton, Pignolet, Silvestre, et al., 2013). n-Hexane at a ratio of 1:4 was used for the extraction of lipids, which were determined gravimetrically. The lipids were extracted three times for a duration of 1 h. The compositional profile of CPI is given in Table 1.

Table 1
Proximate composition (g per 100 g dry matter) and extraction yield (%) of chlorella protein isolate (CPI).

Extraction yield (%)	1.9 ± 0.1
Ash	2.3 ± 0.5
Total carbohydrates	3.4 ± 0.4
Protein	86.8 ± 4.8
Lipids	7.6 ± 4.8

2.2.3. Preparation of the probiotic powders

The probiotic powders were prepared as described in Fortuin et al. (2024) by homogenising an 8 % wt. CPI suspension twice at 800 bar (Panda PLUS 2000; GEA, Parma, Italy) and mixing it with maltodextrin (12 % wt., 15 DE), trehalose (4 % wt.), and glucose (1 % wt.), with all values representing the final concentrations in the suspension. The suspension was stirred until the complete dissolution of solids, adjusted to pH 7 with 0.1 M NaOH, and stored at 4 °C until further use. The prepared CPI formulation was inoculated with freshly harvested LGG cells as described in Hellebois et al. (2023). One mL aliquots of the inoculated formulations were transferred into 24-well cell culture plates (CELLSTAR, Greiner Bio-One, Frickenhausen, Germany) and either non-treated (CNT) (i.e. frozen immediately for 2 h at -80 °C) or fermented (CF) at 37 $^{\circ}\text{C}$ until a pH plateau (pH \approx 4.5) was reached (tpH4.5 = 75 min) and frozen afterwards. The frozen probiotic precursors were lyophilised at -80 °C for 40 h (main stage: 0.120 mbar for 18 h; final stage: 0.010 mbar for 22 h; Martin Christ, Alpha 2-4 LSC plus, Germany).

2.2.4. Physicochemical, thermal and microstructural characterisation of the probiotic powders

2.2.4.1. Protein secondary structure. An Optics Vertex spectrometer (Bruker, Billerica, MA, United States) in the Attenuated Total Reflectance (ATR) mode with a diamond crystal was used for performing the Fourier-Transform Infrared Spectroscopy (FTIR) analyses. The analysis was performed as described in Fortuin et al. (2024). The amide I region (i.e., 1600–1700 cm⁻¹) was deconvoluted using Origin 2019b for the determination of the secondary conformational stage of the protein (Jackson & Mantsch, 1995).

2.2.4.2. Water vapour sorption isotherms. The hygroscopicity of the probiotic powders was determined by means of dynamic vapour sorption (DVS) analysis (DVS discovery, TA Instruments, New Castle, United States). In order to obtain the complete sorption profile, approximately 3 mg of sample was placed in the sample chamber and dried at 0 % RH and 20 $^{\circ}$ C for 60 min. Afterwards, mass differences at various RHs were determined in order to obtain the water sorption of the probiotic powders. Every 180 min, the RH was incremented by 10 %, (ranging from 10 to 90 % RH).

The Guggenheim-Anderson-De Boer (GAB) model (van den Berg & Bruin, 1981) was fitted to the obtained water intake - a_w data (Eq. (1)):

$$X = \frac{X_{m}Cka_{w}}{(1-ka_{w})(1-ka_{w}+Cka_{w})} \tag{Eq. 1} \label{eq:4}$$

where X, X_m , C, k and a_w denote the water content at the equilibrium RH (g $100~g^{-1}$), water content (g $100~g^{-1}$) at the monolayer moisture content, a constant related to the net heat of sorption, a constant correcting the properties of the multilayer molecules and the water activity, respectively. The total surface of the monolayer S_m can be obtained from Eq. (1) as follows (Eq. (2)):

$$S_m \! = \! X_m \frac{1}{M_{H_2O}} \! N_A A_{H_2O} = 3.5 \times 10^3 X_m \tag{Eq. 2} \label{eq:Sm}$$

where X_m , $M_{\rm H2O}$, $A_{\rm H2O}$ and N_A are described as the water content (g 100 g⁻¹) at the monolayer moisture content, the molecular weight of water

(18 g mol $^{-1}$), the surface of a single water molecule (1.06 \times 10 $^{-19}$ m 2) and the Avogadro number (6.023 \times 10 23 molecules mol $^{-1}$), respectively.

2.2.5. Thermophysical properties

Thermogravimetric analysis (TGA) was conducted according to our previous study (Fortuin et al., 2024). A TGA2 STARe system (Mettler Toledo, Zürich, Switzerland) and a heating rate of 5 $^{\circ}$ C min $^{-1}$ from 30 to 800 $^{\circ}$ C were used. As an asset, the first derivative (DTG) of the thermographs was constructed with Origin 2019b.

For Differential Scanning Calorimetry (DSC) measurements, all samples were hermetically sealed in aluminium pans. DSC was performed on a DSC 300 Caliris® Select (Netzsch, Germany) differential calorimeter applying a heating rate of 5 $^{\circ}$ C min $^{-1}$ (1st and 2nd cycles) and 10 $^{\circ}$ C min $^{-1}$ (3rd cycle) in the range of -80 to 150 $^{\circ}$ C. Three heating-cooling cycles were carried out for each sample. The glass transition temperature (Tg) was determined from the heating curve during the second heating cycle.

Thermal mechanical analysis (TMA) of polymer samples was performed under inert atmosphere (He) using a DIL 402 select Expedis dilatometer (NETZSCH, Germany) at a heating rate of 5 $^{\circ}$ C min $^{-1}$, constant load of 0.2 N and in the temperature range from -80 to 150 $^{\circ}$ C.

2.2.6. Scanning electron microscopy (SEM)

A field emission scanning electron microscope (SEM, SU-70, Hitachi, Tokyo, Japan) was used to determine the microstructure of the probiotic powders. The samples were prepared and analysed as described in Fortuin et al. (2024).

2.2.7. In vitro gastrointestinal digestion testing

2.2.7.1. Static in vitro digestion protocol. For the assessment of the colloidal aspects, proteomic and peptidomic profile, amino acids bio-accessibility, as well as the bacteria's viability during in vitro digestion, the INFOGEST v2.0 static in vitro simulated digestion protocol was implemented (Brodkorb et al., 2019). 250 mg of probiotic powder stored at 4 $^{\circ}\mathrm{C}$ and 11 % RH was mixed with 4.75 mL of MilliQ to achieve a food matrix of approximately 5 g.

2.2.7.2. Investigation of the colloidal changes during in vitro digestion. The methods for the determination of the colloidal changes of the probiotic powder by means of microscopy and static light scattering described in Fortuin et al. (2024) were used. The particle size distribution, span and de Brouckere diameter ($d_{4,3}$) of the *in vitro* digesta were investigated by static light scattering using Mastersizer 3000 (Malvern Instruments, Worcestershire, United Kingdom). The refractive indices of the dispersant and CPI were set at 1.33 and 1.47, respectively (Ahmed & Kumar, 2022). The microstructural changes of the protein in the oral, gastric and intestinal digesta were visualised by means of confocal laser scanning microscopy (CLSM, LSM 880, Zeiss Jena, Germany).

2.2.7.3. Proteomic analysis. The proteomic analysis of the food matrix and in vitro gastrointestinal digesta was conducted according to (Fortuin et al., 2025). The proteolysis throughout gastrointestinal in vitro digestion was analysed by means of capillary sodium dodecyl sulfate - polyacrylamide gel electrophoresis (SDS-PAGE). A dispersion of 1 mg mL $^{-1}$ of the probiotic powders in PBS was prepared as the food matrix.10 μL mL $^{-1}$ of β -mercaptoethanol were used to solubilise the proteins present in the food matrix, gastric and intestinal digesta. Moreover, the gastric digesta were diluted 1:1 with PBS. The instructions of a Protein 80 chipkit and a bioanalyser 2100 (Agilent Technologies, Santa Clara, CA, United States) were used for the analysis. The gel reconstruction was performed using Agilent's 2100 Expert software.

In order to determine the primary amino groups in each sample, approximately 30 mg of the food matrix were hydrolysed in Pyrex tubes

(Hach, Loveland, United States) with 1 mL 6 M HCl at 110 $^{\circ}$ C for 24 h. The hydrolysed samples were neutralised with 1 mL 6 M and diluted with MilliQ water to a final volume of 10 mL. The primary amino groups were determined as mentioned in our previous study (Fortuin et al., 2025).

The degree of protein hydrolysis was quantified as follows (Eq. (3)):

DH (%) =
$$\frac{\text{NH}_{2 \text{ digested}} - \text{NH}_{2 \text{ FM}}}{\text{NH}_{2 \text{ total}} - \text{NH}_{2 \text{ FM}}} \times 100$$
 (3)

where DH is the degree of hydrolysis and $\mathrm{NH}_{\mathrm{2figested}}$ and $\mathrm{NH}_{\mathrm{2total}}$ denote the content of primary amino groups in the food matrix, the obtained digesta (gastric or intestinal) and the acidic hydrolysed food matrix.

2.2.7.4. Peptidomic analysis. In order to assess the peptidomic profile of the food matrix (FM) as well as the gastric and intestinal chymes, nanoliquid chromatography-mass spectrometry (nano-LC-MS/MS) was used as described in our previous study with minor modifications (Fortuin et al., 2025). In order to identify the proteins and peptides, the MS/MS files from two technical replicates were merged into a single search. The database UniProt Chlorella vulgaris (11568 sequences) downloaded on August 05, 2024 was used for the identification. The datasets were refined with Progenesis QI for Proteomics software (version 4.2, Nonlinear Dynamics, Waters, Newcastle upon Tyne, UK). The proteomic data were deposited in the ProteomeXchange Consortium via the PRIDE partner repository (S. D. Nielsen et al., 2017; S. D.-H. Nielsen et al., 2023) and is available via ProteomeXchange with identifier PXD066171.

2.2.7.5. Amino acid composition of the probiotic powders and their intestinal in vitro digesta. The methods described in our previous study (Fortuin et al., 2025) were used to quantify the intestinal bioaccessibility of the amino acids. Alanine (Ala), aspartic acid (Asp), cysteine (Cys), glutamic acid (Glu), glutamine (Gln), glycine (Gly), histidine (His), isoleucine (Ile), leucine (Leu), lysine (Lys), methionine (Met), phenylalanine (Phe), proline (Pro), serine (Ser), threonine (Thr), tryptophan (Trp), tyrosine (Tyr) and valine (Val) were quantified by the methyl-chloroformate (MCF) derivatisation method. Asparagine (Asn) and cysteic acid (Cya) were determined by the trimethylsilyl (TMS) derivatisation method. The sum of Cys and Cya represented the total Cys content. Gas chromatography – mass spectrometry (GC (7890 B) – MS (5977 A), Agilent Technologies, Santa Clara, US) equipped with a multipurpose autosampler (MPS, GERSTEL, Mühlheim, Germany) was used to identify the volatile esters present in the derivatised samples. Arginine (Arg) was quantified using an enzymatic kit (Megazyme, K-LARGE 07/20).

2.2.8. Microbiological assessment

2.2.8.1. Quantification of the total viable counts (TVC). The TVC of LGG in the probiotic solutions and powders were quantified according to Fortuin et al. (2024). Therefore, 1 mL of probiotic solution, approximately 250 mg of probiotic powders and 1 mL of digesta were mixed with 9 mL of phosphate buffered saline (PBS) in a stomacher bag (MiniMix 100 W, Interscience, Roubaix, France) and serially diluted. The pour-plate method was used to plate the samples. The plates were incubated at 37 \pm 1 $^{\circ}$ C for 48 h and the colony-forming units (CFU, expressed on a dry basis) were determined with a Scan 500 automatic colony counter (Interscience, Roubaix, France).

2.2.8.2. Storage stability testing. The storage stability of the probiotic powders was investigated as described in our previous study (Fortuin et al., 2024). In order to investigate the impact of temperature on the viability of LGG, the powders were stored in hermetically sealed cabinets at 4, 20 and 37 ± 0.5 °C at a constant water activity (a_w) of 0.11. To

test the influence of the a_w , the powders were stored at $a_w=0.11$ and $a_w=0.75$ at $20~\pm~0.5~^{\circ}\text{C}$, using LiCl and NaCl saturated salt solutions, respectively. The viability of the bacteria was determined as mentioned in section 2.2.8.1. Sampling was conducted at regular time intervals until the bacterial counts declined to approximately 6 log CFU g $^{-1}$.

The Weibull model was fitted to the data in order to determine the cells' inactivation kinetics (Eq. (4)) (van Boekel, 2009):

$$\log S(t) = \frac{1}{2303} \left(\frac{t}{\alpha}\right)^{\beta} \tag{4}$$

where S(t) is defined as the survival ratio S(t) = N(t) N_0^{-1} , t is the corresponding time (days), α is a scale parameter and β denotes the shape parameter.

The shelf-life of the probiotic powders, i.e., the time required for reaching the TVCs minimum (6 log CFU g^{-1}) as established by the FAO/WHO, the following equation was used (Eq. (5)):

$$t_{d} = \alpha \left(\left(-\ln(10^{-d})^{\frac{1}{\beta}} \right)$$
 (5)

where d is the number of decimal reductions, α (days) and β are the Weibull model kinetic parameters as described in Eq. (4).

2.2.8.3. LGG viability during in vitro digestion. A qualitative (CLSM) and quantitative (TVC enumeration) analysis of the viable bacterial cells was performed as described in our previous study (Fortuin et al., 2024). The inactivated and viable bacterial cells present in the oro-gastrointestinal digesta were stained with 1.5 μ L mL $^{-1}$ propidium iodide (20 mM, $\lambda_{Ex}=488$ nm, $\lambda_{Em}=585-640$ nm) and SYTO9 (3 mM, $\lambda_{Ex}=488$ nm, $\lambda_{Em}=498-550$ nm), respectively (LIVE/DEAD BacLight, Thermo Fisher Scientific, Waltham, MA, United States) and analysed by means of CLSM as described in section 2.2.7.2. For the quantification of the TVC of LGG, minimum 3 mL of gastrointestinal digesta (t = 120 min) were mechanically homogenised in a stomacher bag (Minimix 100, Interscience, Roubaix, France), followed by serial dilutions in PBS. The viable LGG cells were enumerated as described in section 2.2.8.1.

2.2.8.4. Cell adhesion properties. For the investigation of LGG's cell adhesion properties to an intestinal epithelium co-culture model, human colon cancer Caco-2 cell line ATCC ref HTB-37 and HT29-MTX cells were seeded on 6-well microplates and eight-chambered microscope slides (Nunc Lab-Tek II, Thermo Fisher Scientific, Waltham, MA, United States). The cells were grown and pre-treated as described in our previous study (Fortuin et al., 2024). Adhered bacterial cells were enumerated as described in Świątecka et al. (2010) with slight modifications. After incubation (t = 120 min, T = 37 \pm 1 $^{\circ}\text{C})$ of the intestinal epithelium with intestinal digesta (V = 2.5 mL and 300 μL for each microwell and LabTek chamber, respectively), the samples were washed twice with PBS. A qualitative investigation of the viable bacteria was conducted by means of CLSM, as described in section 2.2.8.3. For the determination of the TVC of adhered bacterial cells, the intestinal epithelium was diluted with 2.5 mL PBS, scraped off from the microplate and mechanically broken. Afterwards, the viable cells were quantified as described in section 2.2.8.1.

2.3. Statistical analysis

For the identification of the significant differences, the data was subjected to ANOVA followed by Tukey's post hoc means comparison test (p < 0.05). The analysis of the nano-LC MS/MS proteomic and peptidomic datasets were carried out as described in our previous study (Fortuin et al., 2025). After identifying the significant proteins and peptide sequences, the datasets were subjected to hierarchical cluster analysis using the Euclidean distances and Ward's agglomeration methods based on rows (samples) and columns (proteins/peptides relative abundances). ANOVA was conducted using Origin 2019b

(OriginLab, Northampton, MA, USA), PLS-DA was performed using Unscrambler X (Camo, As, Norway) and hierarchical cluster analysis was carried out employing ClustVis web tool (Metsalu & Vilo, 2015).

3. Results & discussion

3.1. Physicochemical, microstructural and thermal characterisation of the probiotic powders

3.1.1. Protein secondary structure

The impact of fermentation on the chemical structure of the probiotic powders was evaluated by FTIR analysis as illustrated in Fig. 1. The spectral pattern of CPI, the free LGG cells and the LGG containing probiotic powders showed the characteristic peaks corresponding to the secondary structure of proteins, i.e., amide I, 1700–1600 cm⁻¹ (C = O stretching vibrations of peptide bonds), amide II, 1500-1600 cm⁻¹ (N-H bending/C-N stretching modes) and amide III, 1200-1400 cm⁻¹, (N-H in-plane and C-N stretching vibrations) regions (Fig. 1A). Moreover, the characteristic peak at 1210–1240 cm⁻¹ – assigned to the asymmetric stretching bands of the phosphodiester groups of nucleic acids (Hlaing et al., 2017) – was found in both free and encapsulated LGG cells. The peak's intensity was reduced in the case of the probiotic powders. indicating the satisfactory embedment of the LGG cells into the wall material, in agreement with the findings reported in our previous study (Fortuin et al., 2024). Additionally, peaks at 1149, 1107, 1078, 1034 cm⁻¹, characteristic of carbohydrates such as maltodextrin, trehalose and glucose, were identified (Hellebois et al., 2023; Kim et al., 2023).

The predominant protein secondary structures were identified by deconvoluting the peaks in the amide I region (1700–1600 cm⁻¹). Three major secondary structure conformations were confirmed, i.e. β-sheet (at $1630-1623 \text{ cm}^{-1}$), α -helix (at $1655-1651 \text{ cm}^{-1}$) and antiparallel β -sheet/aggregated strands (at 1691–1980 cm⁻¹) (Fig. 1B). The predominant conformational structure identified in the isolate and probiotic powders was α-helix (CPI: 78 %, CNT: 68 %, CF: 75 %), followed by β-sheet (CPI: 20 %, CNT: 27 %, CF: 22 %) and aggregated strands (CPI: 2 %, CNT: 5 %, CF: 3 %). Nonetheless, the secondary protein conformational state differences among the tested treatments were nonsignificant. Ladjal-Ettoumi et al. (2024) reported five secondary structure confirmations (β -turns: 33 %, random coils: 28 %, β -sheets: 25 %, α-helix: 13 % and aggregated strands: 11 %, respectively) for CPI extracted by isoelectric point precipitation. It is well-documented that different protein secondary structures can be obtained through different extraction methods, which might explain the differences observed in our study (Hadinoto et al., 2024; Xiao et al., 2024). In their study, Moreira et al. (2025) demonstrated that Chlorella vulgaris protein isolates prepared via different extraction methods, including high pressure

homogenisation coupled with isoelectric precipitation, exhibited a predominant α -helix structure followed by β -sheet secondary structures, which corroborates our findings.

3.1.2. Water vapour sorption properties

For the determination of the residual moisture content, the lyophilisates were transferred to a controlled atmosphere cabinet at RH $=11\,\%$ for 5 days. The fermentation of the lyophilisate precursors led to a significant (p < 0.01) increase in the residual moisture content of the obtained powders, i.e., 6.2 and 7.4 g 100 g $^{-1}$ for the untreated and fermented exemplars, respectively. It is assumed that the observed differences are associated with the presence of secondary metabolites, i.e., organic acids, amino acids or exopolysaccharides, produced during lactic acid fermentation. It should be noted that the measured residual moisture was significantly higher compared to that reported in our previous work (2.1–2.9 g 100 g $^{-1}$, Fortuin et al., 2024), which can be ascribed to the pre-conditioning of the CPI probiotic powders at RH \approx 11 %.

According to the Brunauer's classification, the obtained water vapour sorption isotherms (Fig. 2) can be distinguished as a hybrid of type II and type III water vapour sorption isotherms, which are usually characteristic for the water vapour adsorption of proteinaceous

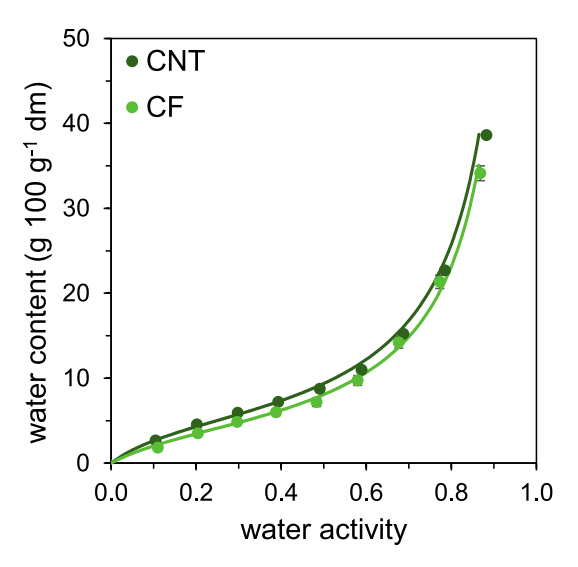


Fig. 2. Water vapour sorption isotherms of fermented (CF) and non-treated (CNT) powders embedding *Lacticaseibacillus rhamnosus* GG fortified with chlorella protein isolate.

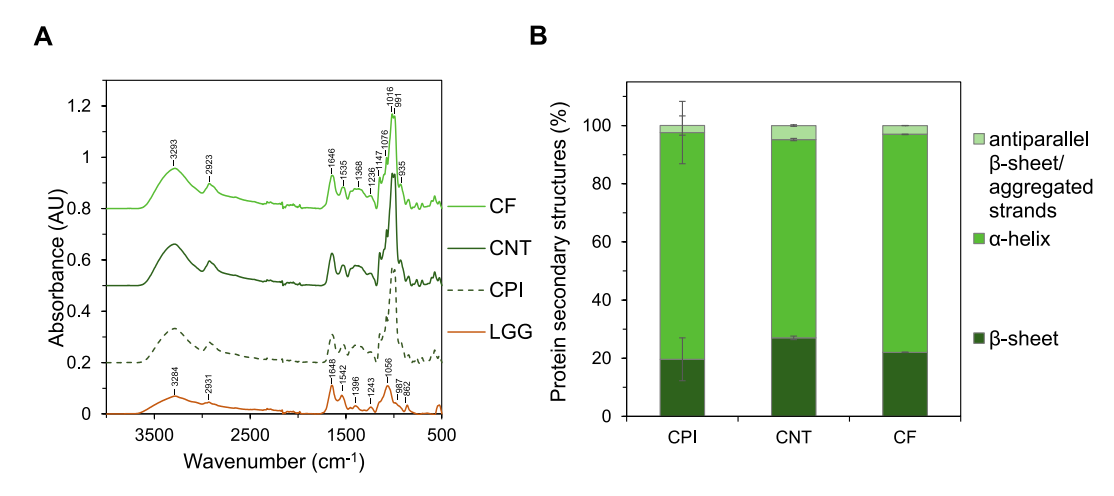


Fig. 1. FTIR spectra (A) and prevalence of the protein secondary structures (B) of probiotic powders embedding *Lacticaseibacillus rhamnosus* GG (LGG) fortified with chlorella protein isolate (CPI) with (CF) and without (CNT) fermentation of the powder precursors.

microporous food matrixes (Lowell & Shields, 1984) and foods rich in soluble sugars, respectively (Al-Muhtaseb et al., 2002). In order to obtain the kinetic parameters describing the water vapour sorption behaviour of the probiotic powders, the GAB model -being valid for both type II and III isotherms - was fitted to the data (Table 2). The fermented probiotic powders exhibited a slightly higher monolayer water content, X_m (p > 0.05), meaning that they convey more water adsorption sites than their non-fermented counterparts. The X_m values determined in this study (5.34 and 5.69 g 100 g⁻¹ for CNT and CF) are in keeping with those reported in our previous (Fortuin et al., 2024) as well as other studies (Hoobin et al., 2013; D. Ying et al., 2012). Nonetheless, the binding of the monolayer water to the surface of the CF wall material was looser as indicated by the calculated Guggenheim constants, i.e. C = 7.19 vs 3.08 for CNT and CF (p < 0.01), respectively. In general, when the water content, m, is below the monolayer level, water molecules are tightly bound to other components, resulting in reduced molecular mobility. This, in turn, enhances the stability of dehydrated matrices by limiting spoilage caused by microbial activity or biochemical reactions. On the other hand, at $m < X_m$, lipid oxidation of the cell membrane bilayer due to oxygen exposure and metal ion activity can accelerate the inactivation of probiotic bacteria cells during storage (Passot et al., 2012). No significant differences were found for constant k (0.999 and 0.972 for CNT and CF, respectively), which suggests a similar multilayer water binding behaviour between the two probiotic powders. The inflexion points of the water vapour sorption determined from the derivatives of the experimental GAB models isotherms ($a_{w,crit} = 0.246$ and 0.171, for CNT and CF, respectively), suggested that the fermented powders are more prone to structural changes and consequently, the loss of the biological activity is higher at lower aw than the non-fermented exemplars.

3.1.3. Microstructure of the probiotic powders

As illustrated in Fig. 3, the CPI-fortified probiotic powders exhibited a compact, flaky, microporous structure with sharp edges, which is comparable to the SEM micrographs of SPI and CPI powders acquired by Ladjal-Ettoumi et al. (2024). A closer investigation (5000 \times) of the surface characteristics of the fermented probiotic powder particulates (Fig. 3B) confirmed their larger micropores compared to their unfermented counterparts (Fig. 3A). The rugged morphology of the CF powders can be ascribed to the non-covalent supramolecular stabilisation of the acid protein aggregates gel network formed during the lactic acid fermentation at pH close to the isoelectric point of Chlorella vulgaris proteins i.e. pI ~4.0-5.5 (Chen et al., 2024; Ursu et al., 2014). Notably, the fermentation of the lyophilisate precursors did not enhance the LGG cells encapsulation efficacy, as many LGG cells were partly embedded in the outer part of the wall material. On the contrary, CNT systems offered a substantially better engrafting of the probiotic cells in the lyophilised particulates - and therefore, a higher lyoprotective and storage stabilising effect.

3.1.4. Thermophysical properties

The thermal stability of the CPI fortified probiotic powders was

Table 2
Influence of pre-cursor treatment (either fermented (CF) or non-treated (CNT)) on the kinetic parameters of the Guggenheim-Anderson-de Boer (GAB) model fitted to the water vapour sorption isotherm data of the probiotic powders fortified with chlorella protein isolate.

	$X_{\rm m}~(g~100~g^{-1})$	C (-)	k (-)	R ² (-)
CNT CF	$\begin{array}{l} 5.34 \pm 0.16^{a} \\ 5.69 \pm 0.47^{a} \end{array}$	$\begin{array}{l} 7.18 \pm 1.23^{a} \\ 3.08 \pm 0.81^{b} \end{array}$	$\begin{array}{c} 0.999 \pm 0.004^a \\ 0.972 \pm 0.013^a \end{array}$	0.999 0.998

 X_m : monolayer water content; C: Guggenheim constant describing the difference between the free enthalpy of the monolayer and liquid water molecules. a,b Different letters between the rows denote a significant difference according to Tukey's post hoc means comparison test (p < 0.05).

assessed by thermogravimetric analysis (Fig. 4, Table 3) following their pre-conditioning under controlled atmosphere (\approx RH 11 %) conditions for 4 days. Three major mass loss events were observed as illustrated in Fig. 4. The first mass loss event occurring at 47 - 57 °C (6.2 < $\Delta m < 7.4$ % wt.) was associated with the evaporation of the residual moisture. The mass loss event at 206-211 °C was attributed to the decomposition of low molecular oligosaccharides (i.e. glucose and trehalose), whereas the substantial powder weight loss at 265–267 °C (48.0 $< \Delta m < 43.2 \%$ wt.) was mainly due to the decomposition of the protein-maltodextrin complexes (Hellebois, Fortuin, et al., 2024). Two additional weight loss events at higher temperatures (not illustrated in Fig. 4), i.e., 474-477 °C (26.0 $< \Delta m <$ 23.8 % wt.) and 650–677 $^{\circ}\text{C}$ (6.2 $< \Delta m <$ 16.4 % wt.) corresponded to the decomposition of the mineral-maltodextrin complexes and the pyrolysis of the residual organic matter. Except for the onset of the water evaporation event, no significant differences in the onset temperatures of the thermal decomposition between CNT and CF were observed.

Previous studies have well-documented that the physical state of wall material (i.e., rubbery or glassy) – as influenced by the composition of the wall material and storage conditions (i.e. temperature and RH) – is of paramount importance for the structural integrity of the embedding wall material and therefore, the preservation of the biological activity of the probiotic cells during storage (Aschenbrenner et al., 2012; Hellebois, Canuel, et al., 2024; Pehkonen et al., 2008). The glass transition temperatures (Tg) of the CPI fortified probiotic powders were determined at different relative humidities (i.e. 0, 11, 23 and 75 %) - representative of the storage trials conditions conducted in the present work (see also paragraph 3.6) – using DSC and TMA. The DSC and TMA measured T_g values were fitted with the Taylor-Gordon model as illustrated in Fig. 5A and B, respectively. According to the Taylor-Gordon model, the T_g (DSC) values for the dry chlorella probiotic powders were estimated at 111.4 and 110.6 °C, whereas the fitted parameters for the solid and water fraction were $k_1 = 5.59$ and 4.98 and $k_2 = 24.3$ and 22.9 for CNT and CF, respectively (Fig. 5A). A similar behaviour was detected in the case of the TMA fitted data with the T_g being estimated at 90.9 and 91.1 °C, k₁ = 0.81 and 0.83 and $k_2 = 2.73$ and 2.75 for CNT and CF, respectively (Fig. 5B). The differences in the calculated Tg values between DSC and TMA are primarily stemming from the measurements' principle, i.e., Tg is detected from the changes in the specific heat capacity and volume expansion/contraction in the case of DSC and TMA, respectively. Our findings suggest that the fermentation did not significantly impact the plasticisation phenomena in the CF probiotic powders. The latter is in line with our previous findings on untreated or fermented probiotic powders fortified with SPI, WPI and pea protein isolate (PPI) (Fortuin et al., 2024). Nonetheless, the Tg values in the CPI probiotic powders were generally higher than their SPI fortified counterparts.

3.2. Colloidal changes during in vitro digestion

The colloidal changes of probiotic powders under static in vitro digestion conditions were tracked down using confocal laser scanning microscopy (CLSM) (Fig. 6A-C1,2) and static light scattering (SLS) (Fig. 6A-C3, Table 4). Upon exposure to artificial oral fluids, the probiotic powders were rapidly disintegrated, yet not fully dissolved, leading to burst release of the LGG cells. As well-illustrated in the CLSM micrographs, no adverse effects on the viability of LGG cells were observed in the simulated oral boluses (Fig. 6A and B). According to the SLS findings, the simulated oral boluses of the fermented probiotic powders exhibited the highest polydispersity, and particles mean size (span = 9.4 and 3.5, $d_{4,3} =$ 48.5 and 5.2 μm for CNT and CF, respectively. tively). This is in line with our previous study reporting that the oral boluses of LGG fermented lyophilisates fortified with SPI, WPI and PPI were characterised by a larger particles mean size due to the inability of the protein aggregates to fully dissolve during the simulated oral processing (Fortuin et al., 2024).

Following gastric in vitro digestion, both fermented and non-treated

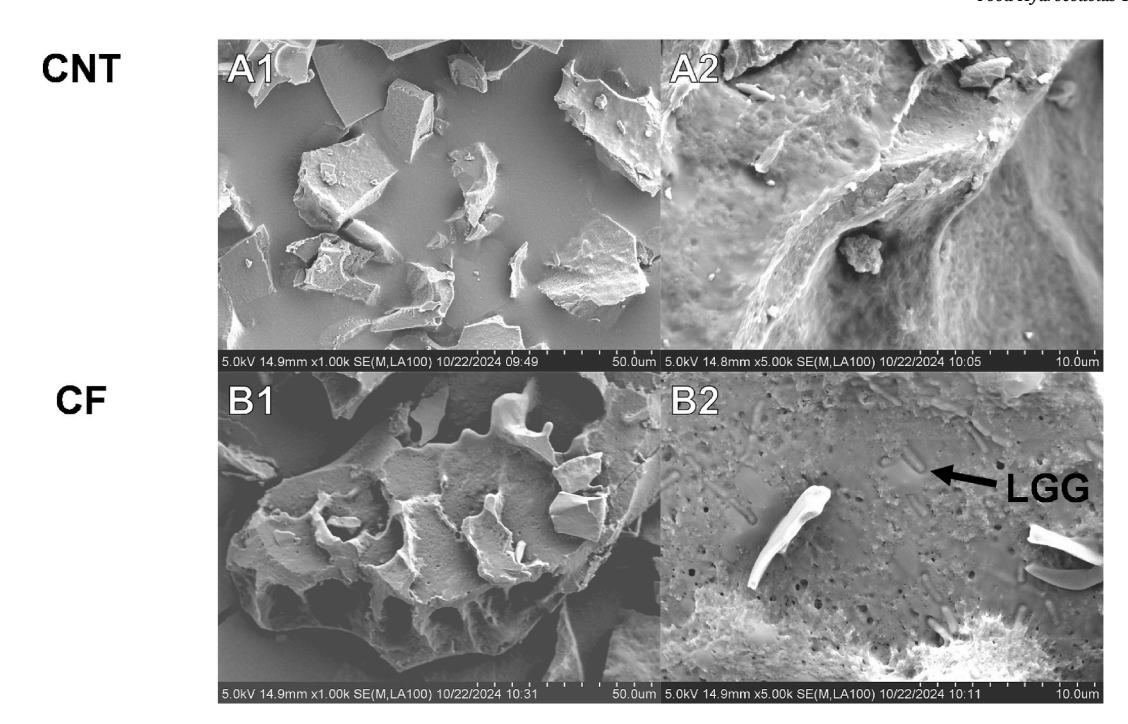


Fig. 3. Scanning electron micrographs of chlorella protein isolate (CPI) fortified probiotic powders encapsulating LGG, prepared from either non-treated (CNT; A) or fermented (CF; B) precursor matrices. Images were captured at magnifications of \times 1000 (1) and \times 5000 (2). CNT powders (A) exhibit a dense, flaky, and microporous surface morphology with sharp edges, whereas CF powders (B) display a smoother, more compact structure with fewer visible pores, suggesting structural densification due to fermentation.

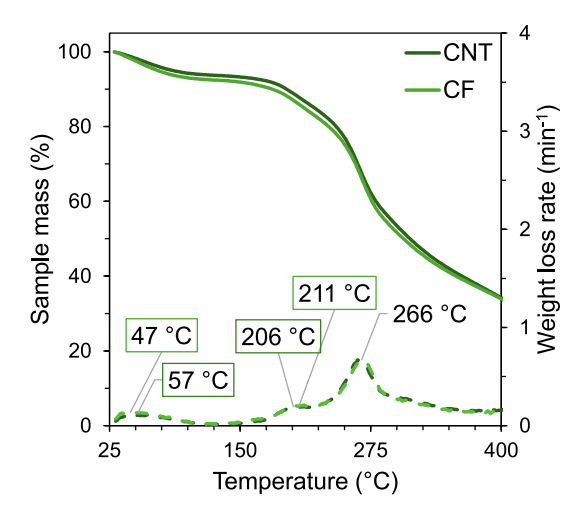


Fig. 4. Thermal properties assessed by TGA (continuous lines) and DTG (dashed lines) of probiotic powders containing LGG cells and chlorella protein isolate, influenced by their precursor treatment (NT = non-treated, F = fermented, C = Chlorella protein isolate).

probiotic powders exhibited a monomodal particle size distribution, with the $d_{4,3}$ being estimated to 27.2 ± 3.1 and $33.6\pm4.6~\mu m$ for CNT and CF, respectively. The obtained mean particle size after gastric in vitro digestion was comparable to that of unfermented (SNT) and fermented (SF) SPI fortified probiotic powders ($d_{4,3}=27.0$ and 23.4 for SNT and SF, respectively) (Fortuin et al., 2025). The increase in the $d_{4,3}$ of the CNT-based gastric digesta suggests that untreated chlorella proteins underwent acid-induced aggregation on their exposure to the simulating gastric fluids. In contrast, the $d_{4,3}$ of CF decreased after gastric digestion as a result of pepsin-induced disintegration. The transformation of protein-rich aqueous systems into colloidal suspensions during gastric processing is largely driven by pepsin- and acid-induced aggregation, along with protein cleavage facilitated by

Table 3Mass loss (%) occurring during different detected thermal events of fermented (CF) and non-treated (CNT) probiotic powders containing *Lacticaseibacillus rhamnosus* GG fortified with chlorella protein isolate.

CNT T (°C)	Mass loss (%)
57 ± 4	6.2 ± 0.1
206 ± 1	7.6 ± 0.4
265 ± 2	48.0 ± 0.7
474 ± 2	26.0 ± 0.6
677 ± 4	12.1 ± 0.5
CF	
T (°C)	Mass loss (%)
47 ± 2	7.4 ± 0.3
211 ± 1	9.1 ± 1.0
267 ± 2	43.2 ± 2.3
477 ± 4	23.8 ± 0.7
650 ± 16	16.4 ± 1.8

pepsin (Loveday, 2022). Due to its complex composition, CPI is characterised by a broad pI ranging from 3 to 5.5 (Ursu et al., 2014), depending on the individual protein classes, and therefore, particulate acid gels can be gradually formed and partially depleted throughout the simulated gastric digestion. Although no significant differences were found in the span of the CNT and CF gastric digesta, a significant reduction in the polydispersity of the CNT gastric digesta compared to the oral boluses was observed (i.e., from 9.4 to 1.6). This reduction was primarily ascribed to limitations in sampling the very large acid aggregates formed upon mixing with the gastric fluids.

As illustrated in Fig. 6C, the particle size distribution pattern of the probiotic powder digesta was similar to that of the simulating intestinal fluids (blend of pancreases and bile salts). This suggests that the increase in the span and $d_{4,3}$ values of the CNT and CF intestinal digesta is susceptible to the presence of the simulating intestinal fluids. As noticed in Fig. 6C, the characteristic particle peak population in the gastric digesta, detected at $\it ca.$ 20 - 25 μm , was shifted to around 10 - 12 μm in the case

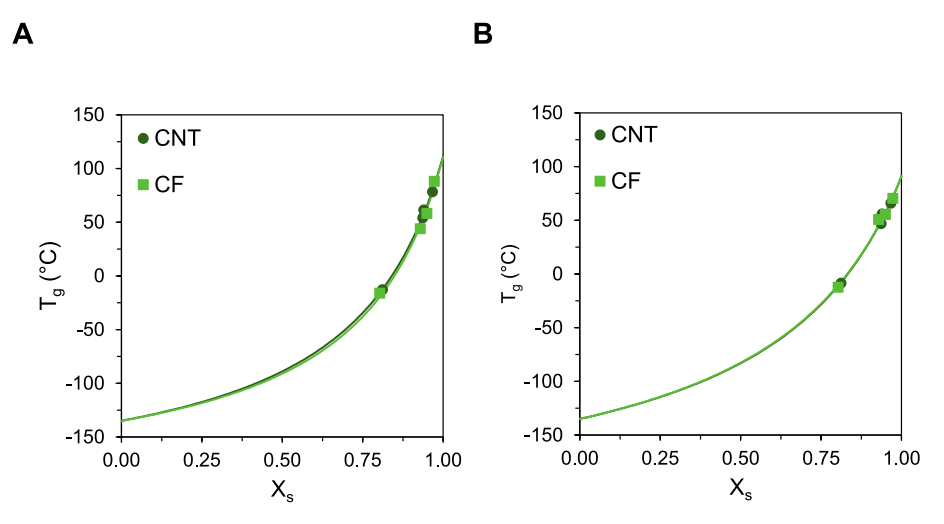


Fig. 5. Glass transition temperatures (T_g) determined by DSC (A) and TMA (B) as a function of solute mass fraction (X_s) for probiotic powders fortified with chlorella protein isolate (CNT = non-treated, CF = fermented). The Taylor-Gordon model was fitted to the data.

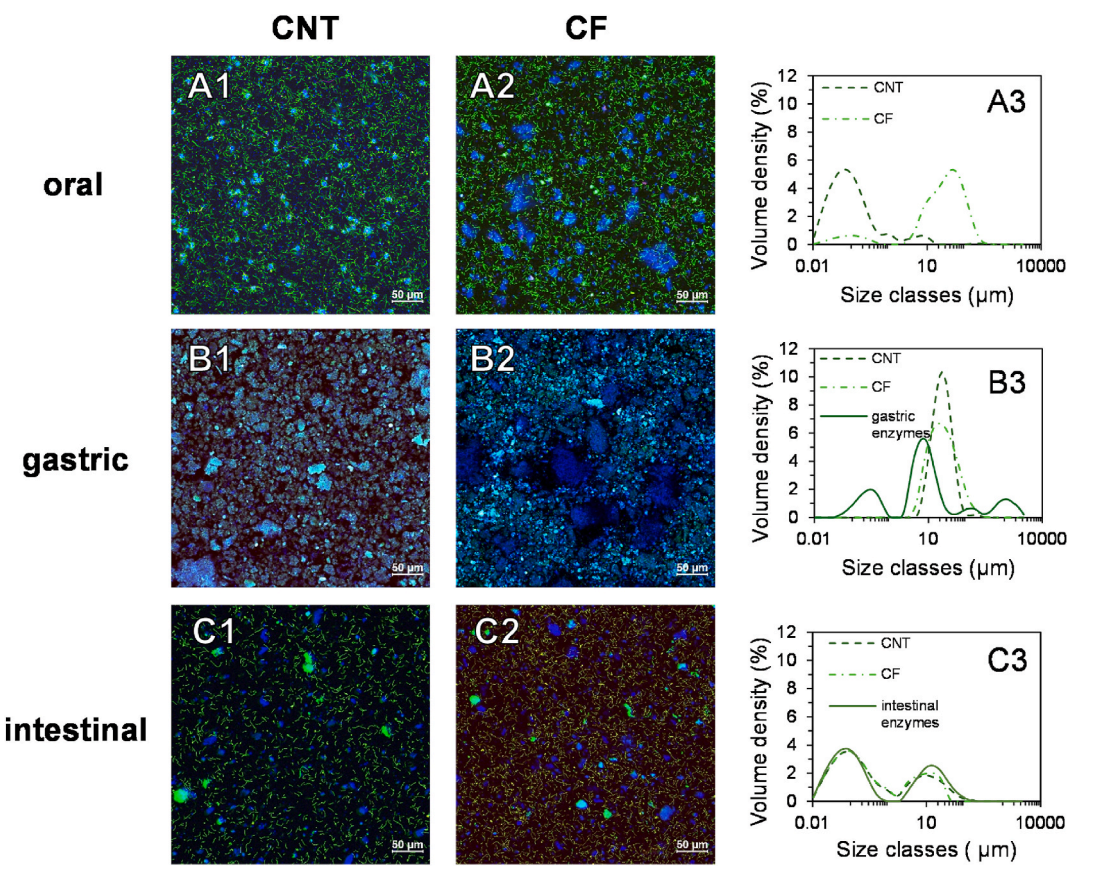


Fig. 6. Colloidal changes investigated by means of CLSM (1,2) and SLS (3) during oral (A), gastric (B) and intestinal (C) static *in vitro* digestion of fermented (CF) and non-treated (CNT) probiotic powders fortified with chlorella protein isolate. Proteins and viable bacterial are shown in blue and green on the CLSM micrographs, respectively. (For interpretation of the references to colour in this figure legend, the reader is referred to the Web version of this article.)

of the intestinal digesta. The peak shift was accompanied by a significant decrease in the volume frequency from 10.7 to 1.9 and 6.8 to 2.1 % for CNT and CF, respectively. In addition, a particle peak population appearing as a shoulder at approximately 0.5–2 μm was exclusively observed in the probiotic powder digesta, confirming the substantial size reduction of the protein aggregates upon their exposure to the pancreatic enzymes. It should be noted that the $d_{4,3}$ values of the CNT and CF intestinal digesta were estimated at 123 and 26.4 μm , which are

comparable, yet higher than those reported in the case SPI, PPI and WPI-fortified probiotic powder intestinal digesta (Fortuin et al., 2024). These findings contribute to the growing body of research focused on the design of food-grade biopolymers capable of self-assembly and adaptive restructuring during gastrointestinal transit, a strategy shown to enhance probiotic protection and delivery. For instance, Madsen et al. (2022) showed that whey protein–alginate complexes reorganise during gastric digestion, initially swelling and later breaking down, while

Table 4 Influence of precursor treatment (either fermented (CF) or non-treated (CNT)) on the volume weighted mean diameter $d_{4,3}$ (µm) and span (dimensionless) of the particles present in the oro-gastrointestinal chymes of probiotic powders containing living *Lacticaseibacillus rhamnosus* GG cells.

	d _[4,3] (μm)			Span (-)	Span (–)			
	oral	G120	I120	oral	G120	I120		
CNT	$\begin{array}{c} 5.2 \pm \\ 2.6^{aA} \end{array}$	$\begin{array}{c} 27.2 \pm \\ 3.1^{\text{bA}} \end{array}$	$\begin{array}{c} 26.4 \pm \\ 0.7^{aA} \end{array}$	9.4 ± 1.6 ^{bB}	$\begin{array}{c} 1.6 \pm \\ 0.1^{aA} \end{array}$	91.3 ± 4.9 ^{cA}		
CF	$\begin{array}{l} 48.5 \pm \\ 14.2^{aB} \end{array}$	$\begin{array}{l} 33.6 \pm \\ 4.6^{aA} \end{array}$	$104.8 \pm 29.3^{\rm bB}$	$\begin{array}{l} 3.5 \; \pm \\ 0.7^{aA} \end{array}$	$\begin{array}{l} 2.9 \pm \\ 0.4^{aB} \end{array}$	$125.3 \pm \\25.6^{\mathrm{bB}}$		

 $d_{4,3}$: de Brouckere mean particle size; G120: gastric digesta after 120 min, I120: intestinal digesta after 120 min. Different letters among the samples denote a significant difference according to Tukey's post hoc means comparison test (p < 0.05). $^{a-c}$ small letters denote a significant difference within one sample. $^{A-C}$ capital letters denote a significant difference between both samples.

cross-linking modulates particle size and digestion resistance. Moreover, Talebian et al. (2022) developed multilayer alginate—chitosan capsules that remained intact in gastric fluid and released LGG in the intestine. These structures mimic physiological triggers, such as pH or enzymatic activity, to create smart delivery systems. The colloidal evolution observed in CPI-based powders suggests that fermented microalgae proteins may offer similar self-assembling properties and, with further optimisation, could serve as functional matrices that respond to digestive cues to protect sensitive probiotics.

3.3. Proteomic and peptidomic profile of the in vitro gastrointestinal digesta

3.3.1. Proteomic profile

Capillary SDS-PAGE was used to determine the extent of the bacterial, pepsin and pancreatin/trypsin-induced protein cleavage of initial and gastrointestinal digesta of the probiotic powders fortified with CPI (Fig. 7A). In general, the intensity and distribution of the SDS-PAGE molecular bands in CPI are known to be impacted by several parameters, including the cultivation technique (Safi et al., 2014) and the protein extraction method (Costa et al., 2024; Ursu et al., 2014). It has been previously shown that growing the microalgal cells under autotrophic conditions promotes the formation of cytoskeleton, chloroplast-related and heat shock proteins of a molecular weight ranging from 12 to 96 kDa (Paterson et al., 2024; Safi et al., 2014). In keeping with the findings of Feng et al. (2025), the electropherograms of the undigested probiotic powders exhibited a smearing background band corresponding approximately to M_w of 10 - 35 kDa, and a high-intensity band corresponding to oligopeptides ($M_W < 3.5 - 6 \text{ kDa}$). The molecular band detected at approximately 15 kDa was ascribed to RuBisCO small subunit, whereas the less pronounced molecular bands detected at 21-39 kDa are related to the presence of peroxiredoxin, Fe-superoxide dismutase and/or photosystem I subunit chloroplast proteins (21 kDa), superoxide dismutase (24 kDa), biotin carboxylase and chlorophyll a/b binding proteins (31 kDa), and ATP synthase subunit beta (39 kDa) (Feng et al., 2025). Noteworthily, only minor differences in the electropherogram pattern between CNT and CF, most probably due to the relatively short duration of the lactic acid fermentation ($t_f = 75 \text{ min}$).

On admixing with the simulating gastric fluids, the broad molecular weight band present at $10-35~\mathrm{kDa}$ was not visible anymore. Solely the bands associated with pepsin and gastric lipase (around $63~\mathrm{kDa}$), as well as the low M_w band representing oligopeptides (i.e., $<3.5-6~\mathrm{kDa}$) could be detected in the electropherograms of the gastric digesta. The electropherograms of the intestinal digesta showed some minor bands at $\sim6.5, 10, 30~\mathrm{and}~60~\mathrm{kDa}$. The band with the highest intensity was visible for oligopeptides (i.e., $<3.5-6~\mathrm{kDa}$) though only minor differences in the pattern of the electropherograms of the CF and CNT intestinal digesta

were detected. Hereby, the observed susceptibility of *Chlorella* sp. proteins to peptic and pancreatic cleavage corroborates other studies (Li et al., 2021; Paterson et al., 2024).

Nano-LC-MS/MS was employed to quantify the proteomes of the FM and gastrointestinal in vitro digesta. The relative abundances of the proteins are illustrated in Fig. 7B. A total of 285 significant proteins were identified in the FM, gastric and intestinal digesta of CNT and CF (Supplementary Excel file). In comparison to our previous study (Fortuin et al., 2025), in which we characterised the proteomic profile of probiotic powders fortified with SPI, PPI and WPI during static gastrointestinal in vitro digestion, a higher number of significant proteins was found for the probiotic powders fortified with CPI. This reflects the complex composition of the chlorella proteome. The most abundant proteins in the FM, as well as the gastrointestinal digesta of both samples, were ribosomal proteins (52-63 %), uncharacterized proteins (25-32 %), as chaperones (5.9-11.5 %). Ribosomal proteins are essential structural and functional components of ribosomes, which are responsible for protein synthesis in cells (Wilson & Cate, 2012), whereas chaperones facilitate the proper folding, assembly, and stability of other proteins without being part of the final functional structure (Hartl et al., 2011). In general, the identified protein classes are in alignment with previous literature findings (Guarnieri et al., 2013).

To compare the proteome similarities of the probiotic powders during in vitro digestion, the proteomic dataset was subjected to hierarchical cluster analysis using the Euclidean distances and Ward's agglomeration methods based on rows (samples) and columns (peptides relative concentration) Fig. 8A. As illustrated in Fig. 8A, the comparison between CNT and CF probiotic powders revealed that CF exhibited a markedly lower abundance of intact proteins compared to their nonfermented counterparts, particularly in the undigested food matrix, indicating substantial pre-digestion by LGG extracellularly expressed proteases. This shift was accompanied by a relative enrichment of ribosomal proteins, enzymes, and membrane proteins, and a depletion of chaperones and uncharacterized proteins, suggesting selective degradation of labile structural components. Across both treatments, in vitro digestion (from food matrix to gastric and intestinal phases) led to a progressive breakdown of sensitive protein classes and a relative persistence of protease-resistant proteins.

The DH, i.e., the free amines released per gram of protein representing the extent of proteolysis during gastrointestinal digestion, is shown in Fig. 7C. The DH in the food matrix (FM) ranged from 0.8 to 1.3 % for CF and CNT, respectively. The values were comparable to probiotic formulations fortified with WPI and lower compared to formulations fortified with SPI, which we reported in our previous study (Fortuin et al., 2025). The differences in the DH rates of the food matrices might be explained by the selectivity of lactic acid bacteria for specific proteins with an open molecular structure (Kieliszek et al., 2021). The differences in the protein secondary structures, which are rather defined by a higher percentage of α-helices in comparison to proteins present in spirulina, might explain the selectivity (Fortuin et al., 2024). No significant difference (p > 0.05) in the DH rates of the pre-fermented vs. non-treated powders was found, which might be explained by the high microbial load of LGG (\sim 10 log CFU g⁻¹). Upon gastric digestion, the DH rates increased to 20.1 and 20.7 % for CNT and CF, respectively. Following intestinal in vitro digestion, the number of free amino groups increased to 87.0 and 83.3 % for CNT and CF, respectively. Interestingly, no significant difference (p > 0.05) regarding the pre-treatment of the probiotic powders was found for the DH determined in the in vitro gastrointestinal chymes. The reported DH values determined in the intestinal digesta are higher in comparison to literature findings, i.e., 17-75 % (Morris et al., 2008). It must be noted that different analytical techniques to determine the DH, different digestion models and strains were used in the mentioned publications. Moreover, they focused on the DH of the whole biomass instead of the protein isolate, which has an impact on the accessibility of the intracellular proteins to digestive enzymes.

J. Fortuin et al.

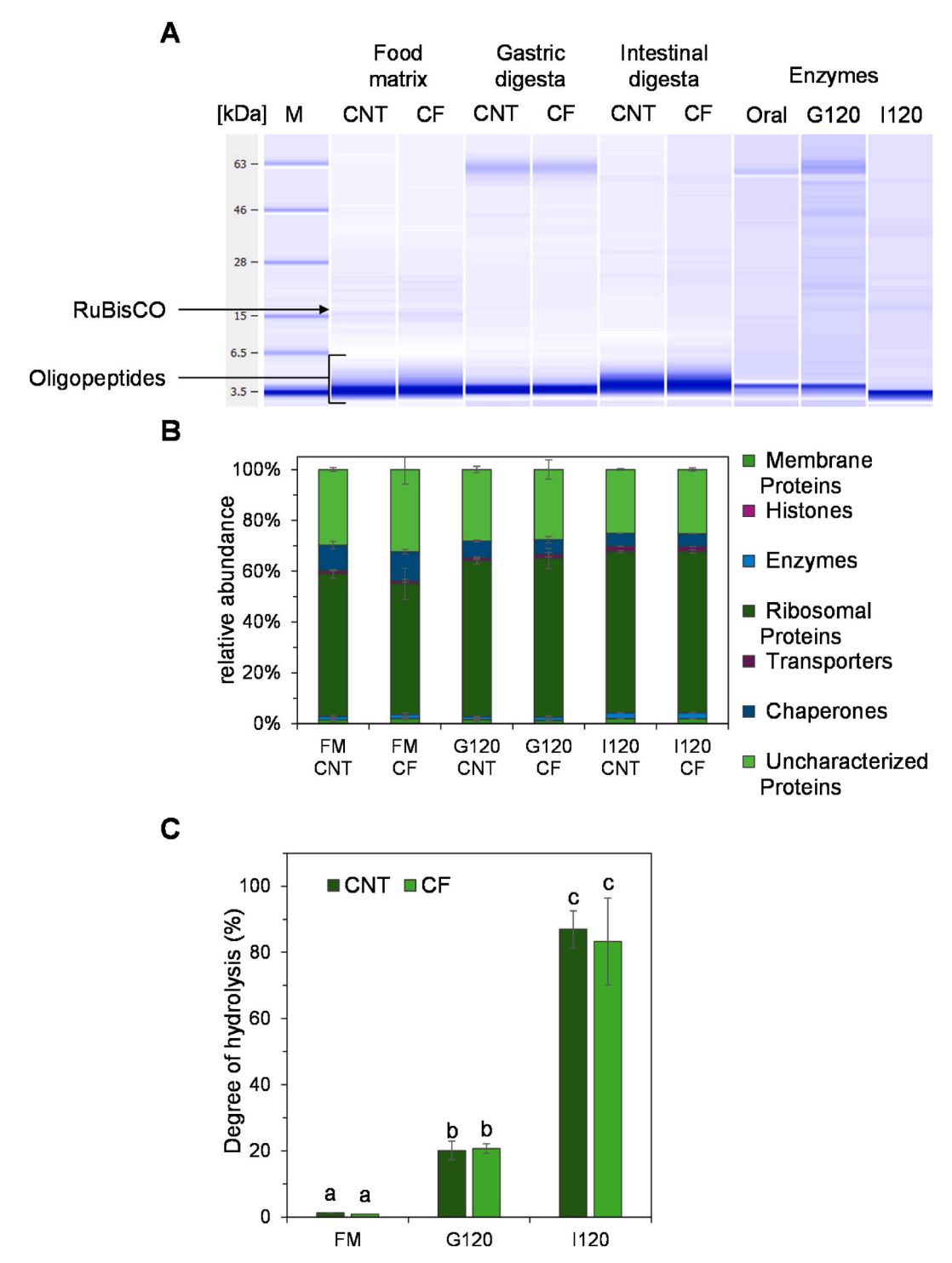


Fig. 7. Capillary SDS-PAGE electropherograms (A), relative protein abundances determined by nano LC-MS/MS (B) and degree of hydrolysis measured by the OPA assay (C) of fermented (CF) and non-treated probiotic powders (CNT) fortified with chlorella protein isolate before and after static *in vitro* gastrointestinal digestion (FM = food matrix, G120 = gastric digesta after 120 min, I120 = intestinal digesta after 120 min, M = molecular marker). $^{a-c}$ Different letters denote a significant difference according to Tukey's post hoc means comparison test (p < 0.05).

3.3.2. Peptidomic profile

A hierarchical cluster analysis heatmap was generated to illustrate the peptidomic profile of the pre-fermented and non-treated probiotic powders during static *in vitro* digestion (Fig. 8B). As illustrated in Fig. 8B, fermented samples (CF) exhibited a higher proportion of short peptides (\leq 5 amino acids) at the undigested (FM) stage, indicating substantial proteolysis by microbial proteolytic enzymes prior to the acid hydrogel lyophilisation. In contrast, non-fermented samples (CNT)

retained longer peptides (≥ 12 amino acids) in early phases, reflecting limited proteolysis during the preparation of the lyophilisate precursors. As digestion progressed from gastric to intestinal stages, both treatments showed a shift toward shorter peptides, though this trend was more pronounced in CF samples. Peptides derived from ribosomal proteins, enzymes, and membrane proteins increased in relative abundance during digestion, whereas those from chaperones and uncharacterized proteins declined, particularly in fermented samples. These changes

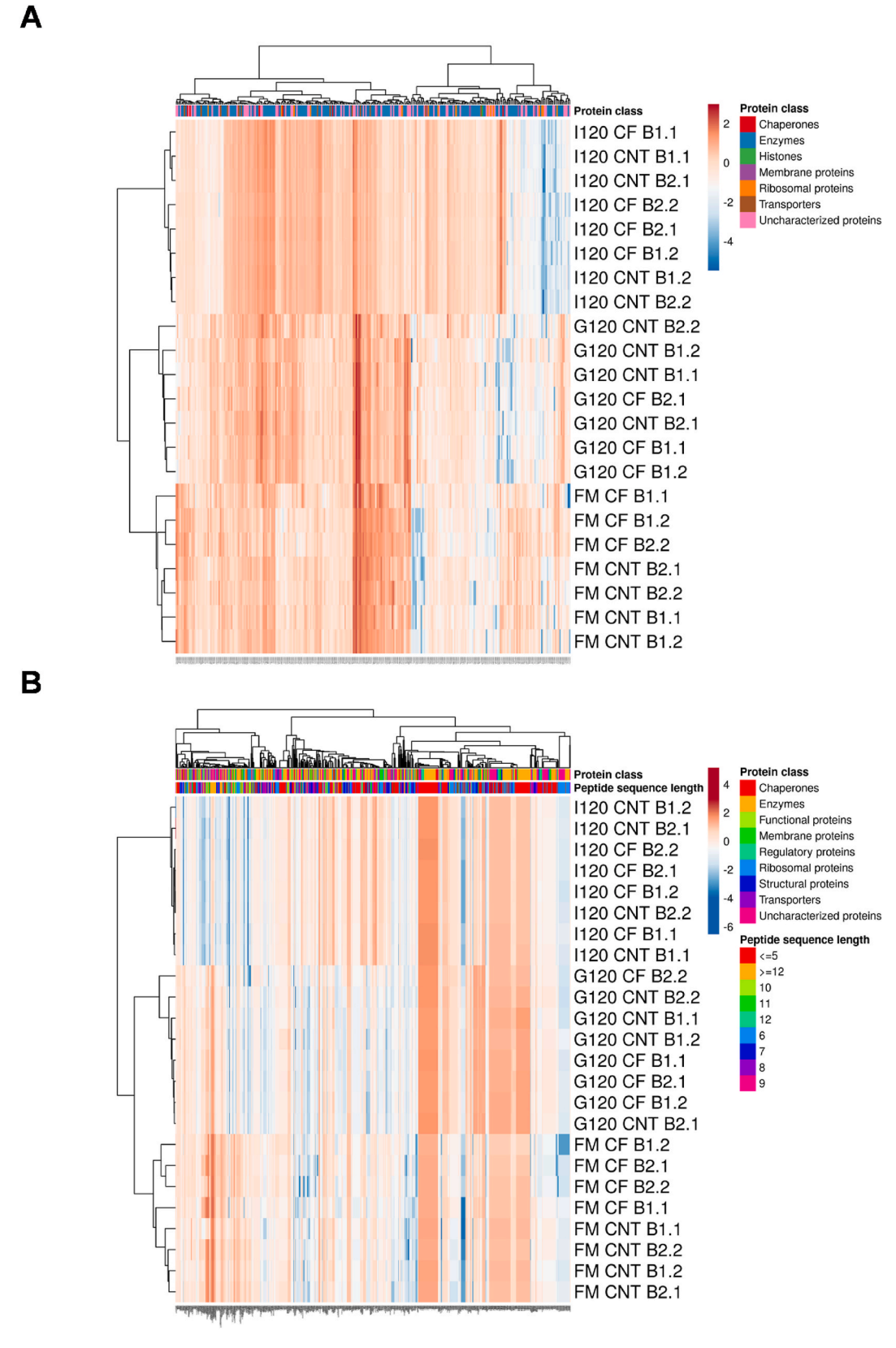


Fig. 8. Hierarchical cluster analysis heat map with dendrograms analysing the effect of precursor treatment (CNT = non-treated, CF = fermented) on the abundance of proteins (A) and peptides (B) detected in the food matrix (FM), *in vitro* gastric (G120) and intestinal (I120) digesta of probiotic powders fortified with chlorella protein isolate.

suggest that fermentation not only enhances proteolytic breakdown but also alters the composition and structural origin of peptides, generating a more diverse and potentially more bioaccessible peptidome.

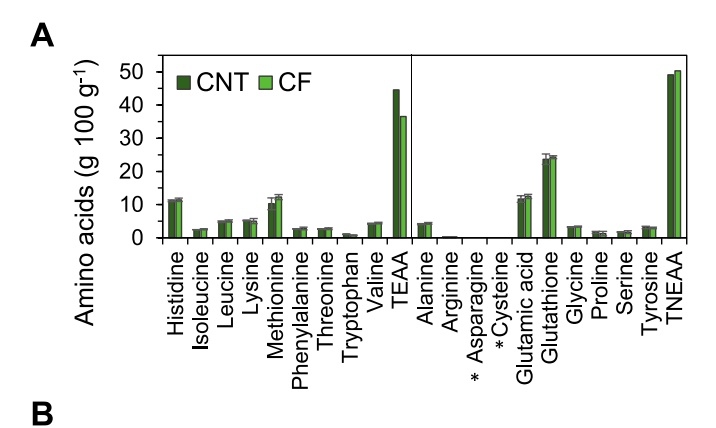
3.4. Initial and intestinal amino acid content

Fig. 9 illustrates the initial (Fig. 9A) and intestinal (Fig. 9B) amino acid content of the probiotic powders. The most abundant amino acids were glutathione (24.3 and 23.6 g 100 g⁻¹), glutamic acid (12.5 and $11.7 \text{ g } 100 \text{ g}^{-1}$), and methionine (12.3 and 10.3 g 100 g⁻¹) and histidine (g 100 g⁻¹), with CF exhibiting higher values than CNT. All essential amino acids (EAA) were identified, with the total EAA (TEAA) content being significantly (p < 0.05) higher in CNT than CF (44.6 vs. 36.5 g 100 g^{-1}). In contrast, the total non-essential amino acid (TNEAA) content was comparable between CNT and CF (50.4 vs. 49.1 g 100 g^{-1}). The observed amino acid composition is keeping with the literature reports; however, variations in extraction techniques, bacterial strains, and amino acid quantification methods may account for differences in measured values (Morris et al., 2008; Mosibo et al., 2024; Paterson et al., 2024). As illustrated in Fig. 9B, the intestinal amino acid content of TEAAs and TNEAAs ranged from 15.2 to 15.7 g 100 g⁻¹ and from 13.01 to 15.2 g 100 g⁻¹ for CNT and CF, respectively. Among all detected AAs, His (5.7 and 6.0100 g^{-1} for CNT and CF, respectively), Gly (3.2 g 100 g⁻¹ for CNT and CF) and Glu (3.1 g 100 g⁻¹ for CNT and CF) exhibited the highest bioaccessibilities.

3.5. Viability of LGG during processing, storage and in vitro digestion

3.5.1. Lyostabilising potential of chlorella protein isolate

The total viable counts (TVC) and losses of LGG during lyophilisation are shown in Fig. 10. In general, the TVC ranged from 10.02 to 10.09 log CFU $\rm g^{-1}$ after lyophilisation for the non-treated and fermented probiotic powders. In agreement with our previous study (Fortuin et al., 2024),



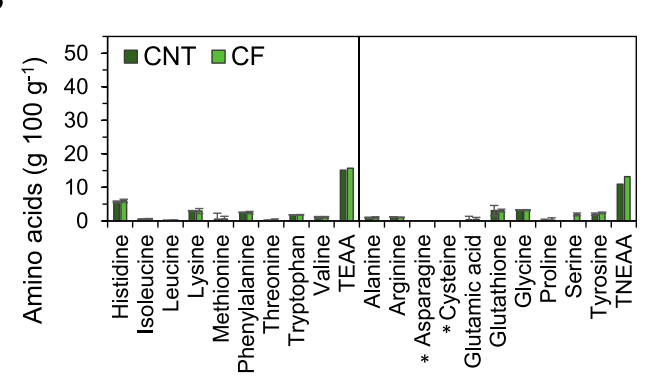


Fig. 9. Initial (A) and intestinal (B) amino acid content of the pre-fermented (CF) and non-treated (CNT) probiotic powders fortified with chlorella protein isolate. *not detected.

fermenting the precursors induced a significantly higher loss rate during lyophilisation (-0.02 vs. -0.10 log CFU g⁻¹, p < 0.01). The losses observed in our previous study were higher, ranging from -0.07 to -0.70 for non-treated and fermented powders, respectively. In comparison to other studies (Pehkonen et al., 2008; D. Y. Ying et al., 2010), the viability of LGG was either higher or similar prior to lyophilisation in this study. Fermentation of the precursors may induce alterations in the phospholipid bilayer of the probiotic cells due to the metabolic activity of the probiotic bacteria, potentially increasing cell vulnerability during lyophilisation (Cui et al., 2018). It is postulated that the better lyostabilising potential of CPI found in the present work compared to the SPI, PPI and WPI counterparts (Fortuin et al., 2024) is associated with the shorter fermentation time ($t_{pH4.5} = 70$, 90, 90 and 240 min for CPI, SPI, PPI and WPI, respectively), leading to lower sub-lethal cellular stress throughout cryogenic processing and lyophilisation. In this study, the difference between the residual moisture and monolayer water (X_m) content was greater for the fermented probiotic powders compared to the non-treated powders (2.6 vs. 0.9). This suggests that, in the fermented powders, water occupied fewer binding sites, possibly due to the structural changes caused by fermentation. It is also plausible that oxvgen reacted with available binding sites, further compromising cell integrity and contributing to higher lethality during lyophilisation. This observation aligns with the higher cell lethality reported in our previous study (Fortuin et al., 2024), where the difference between X_m and residual moisture content was more pronounced compared to the current findings (2.1-3.0). These results indicate that the increase in cell lethality could be linked to the reduced water-binding capacity, leading to enhanced oxidative damage and reduced protection during the freeze-drying process.

3.5.2. Storage trials testing

To investigate the shelf-life aspects of the probiotic powders, accelerated storage trials under controlled RH (RH \sim 11 and 75 %) and temperature (T = 4, 20 and 37 $^{\circ}$ C) were conducted. The Weibull model (Eq. (4)) was fitted to the obtained TVC - storage time data and the parameters α (characteristic time – in days) and β (dimensionless) were calculated (Fig. 11, Table 5). Due to the high survivability of LGG stored at chilling conditions (4 $^{\circ}$ C and 11 % RH), the inactivation kinetics could not have been obtained by neither fitting the Weibull model nor firstorder kinetic model. The obtained kinetic parameters α and β denote the time required for a log (1/e) decline in the living cell's load to be achieved (a) and an indication of the cells' adaptation to the applied stressor (β < 1) or the accumulated cellular damage (β > 1) (van Boekel (2002). According to ANOVA results, α was significantly influenced by the storage temperature (p < 0.01), RH (p < 0.01) as well as the pre-fermentation of the precursors (p < 0.001). In particular, an elevation in the storage temperature and RH α as well as the pre-fermentation of the lyophilisate precursors decreased α . In contrast, only the elevation of the temperature (p < 0.01) and the pre-fermentation step (p < 0.05) significantly decreased the parameter β . Moreover, the fact that $\beta > 1$ in case of both samples, indicates the cumulated damage in the bacterial cells, which increased the lethality of the cells.

Several factors like water vapour adsorption, temperature fluctuations, as well as the ageing of the surrounding wall material may result in changes in the physical state (i.e., glassy to rubbery state transition) of the probiotic powders. These external conditions are likely among the key contributors to cell death over time (Aschenbrenner et al., 2015; Capozzi et al., 2016; Flach et al., 2018; Mendonça et al., 2022; Wang et al., 2025). Conditions regarding the cell, such as the growth phase, pH and ionic strength of the solution and the adaptation ability of the bacterial cells towards temperature and RH conditions are playing also a significant role (van Boekel, 2002). In order to evaluate the impact of the changes in the physical state on the bacterial sublethality, the $T_{\rm g}$ of the probiotic powders was determined as mentioned in section 2.2.5. Samples stored at RH 11 % were still in the glassy state, since $T_{\rm g} > T_{\rm storage}$. In contrast, the physical state of samples stored at RH 75 % was

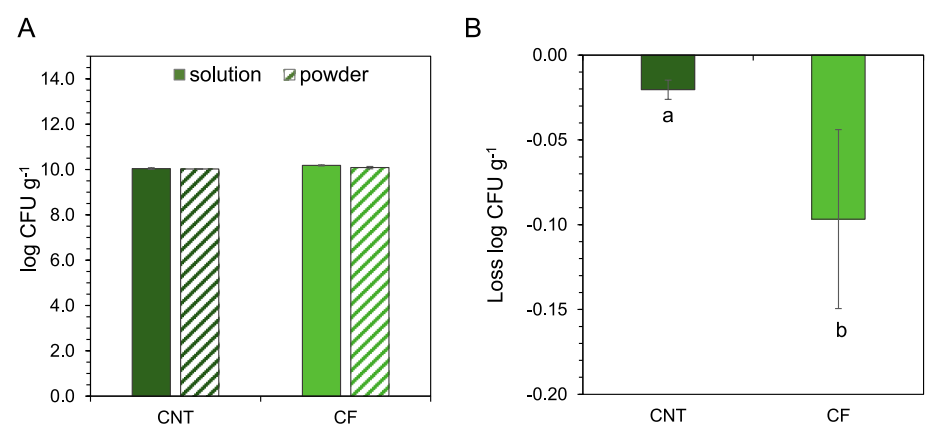


Fig. 10. Influence of pre-cursor treatment on the total viable counts (A) and loss (B) of *Lacticaseibacillus rhamnosus* GG during lyophilisation (NT = non-treated, F = f fermented, C = f chlorella protein isolate). a,b Different letters denote a significant difference according to Tukey's post hoc means comparison test (p < 0.05).

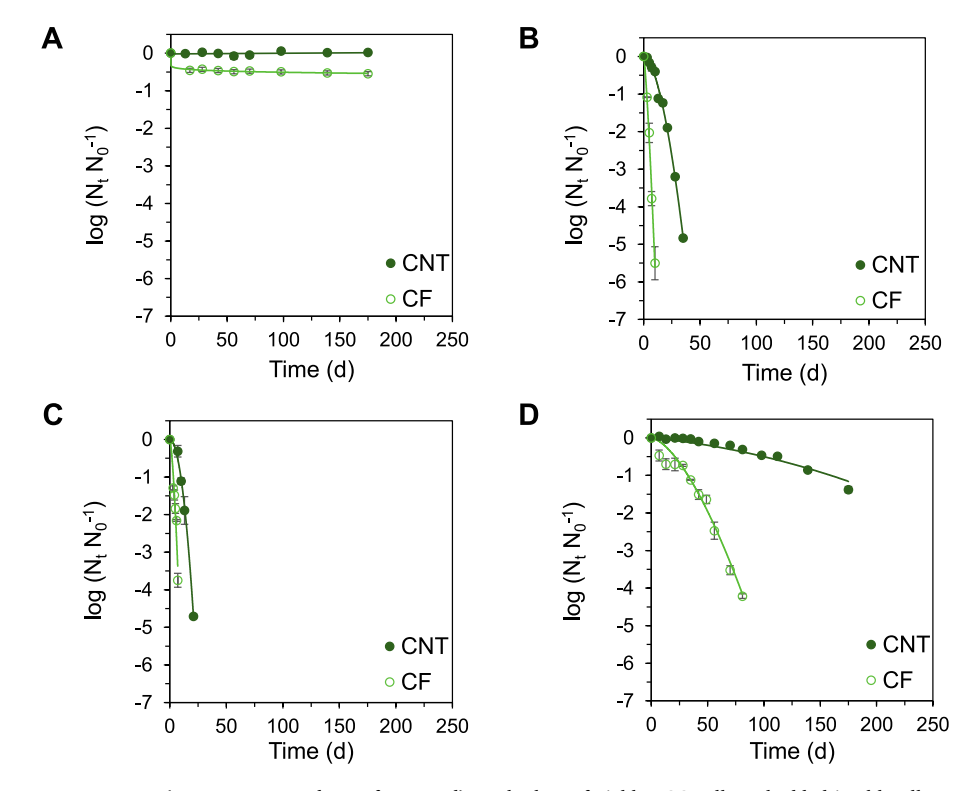


Fig. 11. Influence of precursor treatment (NT = non-treated, F = fermented) on the loss of viable LGG cells embedded in chlorella protein isolate (C = chlorella protein isolate) under controlled storage conditions (A: T = 4 $^{\circ}$ C, $a_w = 0.11$; B: T = 37 $^{\circ}$ C, $a_w = 0.11$; C: T = 20 $^{\circ}$ C, $a_w = 0.75$; D: T = 20 $^{\circ}$ C; $a_w = 0.11$). The modelling of the LGG cells inactivation kinetics was based on the Weibull model (Eq. (1)).

Table 5 Kinetic parameters α (in days) and β (dimensionless) obtained from the Weibull model (Eq. (1)) influenced by the storage conditions (water activity (a_w) and temperature) on the inactivation of *Lacticaseibacillus rhamnosus* GG cells in powders fortified with chlorella protein isolate either non-treated (CNT) or fermented (CF) prior lyophilisation.

	a_{w} 0.11									$a_w 0.75$		
	4 °C			20 °C			37 °C		20 °C			
	α	β	adj. R2	α	β	adj. R2	α	β	adj. R2	α	β	adj. R2
CNT CF	nd ^a nd ^a	nd ^a nd ^a	nd ^a nd ^a	$\begin{array}{c} 100.0 \pm 1.8^{dC} \\ 18.0 \pm 1.6^{cB} \end{array}$	$\begin{array}{l} 2.1\pm0.1^{dB} \\ 1.5\pm0.1^{bA} \end{array}$	0.990 0.965	$\begin{array}{c} 9.0 \pm 0.1^{b} \\ 1.5 \pm 0.1^{a} \end{array}$	$\begin{array}{c} 1.8 \pm 0.0^c \\ 1.3 \pm 0.0^a \end{array}$	0.994 0.989	$\begin{aligned} 6.5 &\pm 1.1^A \\ 1.8 &\pm 0.4^A \end{aligned}$	$\begin{array}{c} 2.1\pm0.3^B\\ 1.5\pm0.3^A\end{array}$	0.993 0.907

Different letters among the samples denote a significant difference according to Tukey's post hoc means comparison test (p < 0.05). a^{-c} small letters denote a significant difference within the samples stored at different temperatures. A^{-C} capital letters denote a significant difference depending on the water activity.

^a Not determined.

rubbery, as $T_g < T_{storage}$. Elevating the storage RH and thus changing the physical state of the samples resulted in an acceleration of LGG's death kinetics. These findings are in alignment with previously reported studies (Fortuin et al., 2024; Hellebois, Canuel, et al., 2024; Hellebois, Fortuin, et al., 2024). The pre-fermentation step of the probiotic solutions played a significant role in increasing bacterial cell lethality during storage. A similar phenomenon was observed in our previous study using SPI, PPI, and WPI to fortify probiotic powders (Fortuin et al., 2024). This effect may be attributed to changes in membrane fatty acid composition as an adaptation to acidic conditions, along with alterations in the physical state of membrane lipids. These changes likely resulted in cumulative cell damage during freeze-drying, making the fermented bacterial cells more vulnerable to storage conditions and ultimately increasing lethality.

The shelf-life of the probiotic powders is shown in Table 6. When stored at 20 °C and 11 % RH, the shelf-life ranged from 79 to 294 days, which is shorter than that of probiotic powders fortified with SPI, PPI, and WPI as reported in our previous study (151-348 days) (Fortuin et al., 2024). Compared to non-treated probiotic powders fortified with SPI (SNT), CNT exhibited a similar storage duration. In contrast, fermented samples showed a reduced shelf-life, with CF displaying the shortest duration. Storing the probiotic powders at 11 % RH under cool conditions (4 °C) extended their shelf-life to over two years, based on rough estimations using first-order inactivation kinetics. However, increasing RH and storage temperature significantly reduced shelf-life to 7-19 days and 7-31 days, respectively. A comparison of probiotic powders fortified with SPI and CPI revealed that CPI-fortified powders had a shorter shelf-life when stored at elevated temperatures (37 °C and 11 % RH). This reduction in shelf-life may be attributed to differences in the residual lipid content of the protein isolates, i.e., 3.7 % in SPI and 7.6 % in CPI. The higher lipid content in CPI may promote lipid oxidation in the LGG phospholipid cell wall when stored at 37 °C, further accelerating degradation.

3.5.3. LGG viability during in vitro digestion

The sublethality kinetics plots of LGG during simulated gastrointestinal in vitro digestion is illustrated in Fig. 12. As shown, free LGG cells exhibited significant lethality during gastric (-2.8 log CFU g⁻¹) and intestinal (-3.1 log CFU g⁻¹) digestion, aligning with our previous findings (Fortuin et al., 2024) and emphasizing the importance of embedding cells within the developed formulation for enhanced protection. Upon exposure to gastric fluids, LGG viability decreased, with CNT and CF showing significantly different reductions of 1.3 and 1.8 log CFU g⁻¹, respectively. Based on the results regarding the colloidal changes of the probiotic powders during gastric digestion, it can be hypothesized that the acid-induced protein aggregation entrapped the probiotic cells and limited the exposure to digestive enzymes and low pH (Loveday, 2022; Mulet-Cabero et al., 2019). As noted in our previous study (Fortuin et al., 2024), fermentation time influences the adaptation of probiotic bacteria to acidic environments. For probiotic powders fortified with WPI, a fermentation time of 4 h, reaching a pH of 4.5, allowed LGG cells to gradually adapt to acidity, reducing lethality during gastric digestion (-0.62 log CFU g⁻¹). In contrast, CF underwent

 $\label{thm:continuous} \textbf{Table 6} \\ \textbf{Impact of water activity (a_w) and temperature on the shelf-life (days) of probiotic powders fortified with chlorella protein isolate embedding \textit{Lacticaseibacillus rhamnosus} \ GG \ either \ non-treated \ (CNT) \ or \ fermented \ (CF) \ prior \ lyophilisation.$

	Shelf-life (days)	Shelf-life (days)				
	a _w 0.11	a _w 0.11				
	20 °C	37 °C	20 °C			
CNT CF	$\begin{array}{c} 294\pm13.5\\ 79\pm0.1\end{array}$	$\begin{array}{c} 31\pm0.1\\ 7\pm0.4 \end{array}$	$19\pm0.1\\7\pm0.5$			

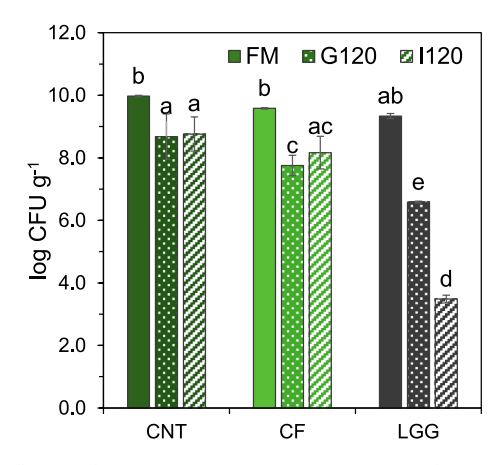


Fig. 12. Influence of precursor treatment (CNT = non-treated, CF = fermented) on the total viable counts of *Lacticaseibacillus rhamnosus* GG cells (LGG) embedded in probiotic powders fortified with chlorella protein isolate throughout gastrointestinal *in vitro* digestion (FM = food matrix, G120 = gastric digesta, I120 = intestinal digesta). $^{\rm a,b}$ Different letters denote a significant difference according to Tukey's post hoc means comparison test (p < 0.05).

fermentation for ~75 min, which may explain the higher LGG cell lethality compared to the WPI-fortified powders. Additionally, changes in membrane fatty acid composition and membrane lipid structure due to acid exposure during fermentation may have led to cumulative damage, reducing LGG resistance to gastric acidity and digestive enzymes. Another factor influencing LGG survival during gastrointestinal digestion is its affinity for adhering to specific proteins, such as whey proteins (Guerin et al., 2018). However, the adhesion affinity of LGG to CPI remains unknown and will be investigated in future research. Comparing LGG sublethality in CNT and CF to powders derived from another microalgal species, Arthrospira platensis (spirulina) (Fortuin et al., 2024), revealed that CNT exhibited lower LGG losses during gastric digestion compared to non-treated spirulina-based probiotic powders (SNT) (-1.3 vs. -1.6 log CFU g $^{-1}$). Conversely, CF showed slightly higher sublethality than spirulina-based pre-fermented powders (SF) $(-1.8 \text{ vs.} -1.6 \log \text{CFU g}^{-1})$.

Following intestinal in vitro digestion, the viability of LGG cells remained unaffected by the simulating intestinal fluids, including bile salts and enzymes, in both probiotic powders (p > 0.05). Compared to CNT, LGG viability in CF powders showed a significant increase after digestion (0.1 and 0.4 log CFU g⁻¹ for CNT and CF, respectively). A similar increase in viable cells post-intestinal digestion was also observed in our previous study (Fortuin et al., 2024). Exposure to bile salts can have detrimental effects on probiotics, including increased cell wall permeability, oxidative stress, DNA damage, protein denaturation, and intracellular acidification (Mendonça et al., 2022). However, probiotics have evolved various stress-response mechanisms to counteract these effects. One key adaptation is the expression of bile salt hydrolases (BSH), which catalyse bile acid hydrolysis, providing glycine and taurine as nutrients for bacterial metabolism (De Boever et al., 2000; Foley et al., 2021). The ability of LGG to express BSH is well established (Hernández-Gómez et al., 2021; Koskenniemi et al., 2011). Additionally, fermentation may enhance BSH expression, as reported by Gil-Rodríguez and Beresford (2021) in certain lactic acid bacteria, which could explain the growth-promoting effect observed in fermented probiotic powders. Other stress-response mechanisms include the bile efflux pump, superoxide dismutase, chaperone proteins, and regulation of the glycolytic pathway (Ruiz et al., 2013).

3.6. Adhesion of LGG to an in vitro intestinal epithelium

A mucin-producing in vitro co-culture gut epithelium model (Caco-2/HT-29-MTX) was used to assess the ability of bacterial cells to adhere to

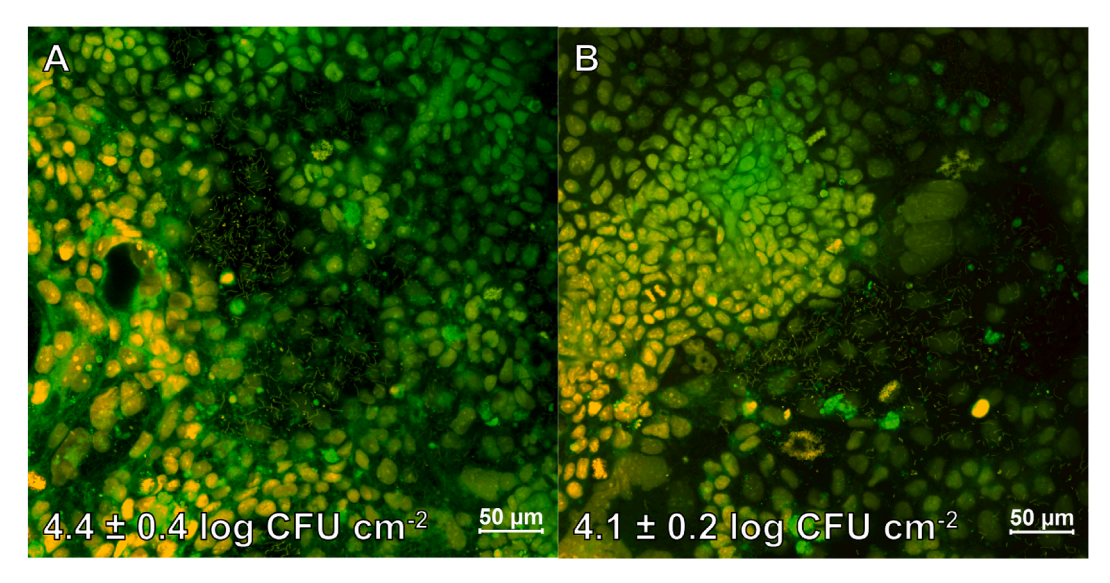


Fig. 13. CLSM micrographs (× 20) illustrating *Lacticaseibacillus rhamnosus* GG cell adhesion to the mucus layer of a gut epithelium co-culture model incubated with intestinal chymes of probiotic powders fortified with chlorella protein isolate and different precursor treatment (either non-treated (A) or fermented (B)). Living cells are represented by green colour, dead cells by red.

mucosa layer of human gut epithelium. CLSM micrographs (Fig. 13) revealed a substantial number of cultivable adhered LGG cells (4.4 and 4.1 log CFU cm⁻²) in CNT (Fig. 13A) and CF (Fig. 13B), respectively. These values are generally comparable to those reported in the case of WPI and PPI (i.e., 4.40 and 4.27 log CFU cm⁻², respectively) but significantly higher than SPI (i.e., 3.89 log CFU cm⁻²) (Fortuin et al., 2024). In keeping with our previous study, the pre-fermentation of the lyophilisate precursors did not affect significantly the adhesion of the LGG cells to the mucosa of the in vitro co-culture gut epithelium model. It was previously shown that the adhesion of probiotic cells to the gut mucosa is mediated by the molecular interactions between the glycocalyx and bacterial cell surface components such as adhesins, lipoteichoic acid, surface layer associated proteins and pili (Monteagudo-Mera et al., 2019). In this context, both the food matrix components and probiotic strain are known to influence bacterial adhesion to the intestinal epithelium (Flach et al., 2018; Tallon et al., 2007). As concerns intact proteins and their peptic/pancreatic cleaved derivatives, previous studies associated their gut epithelium adhesion capacity with their influence on the expression of adhesion proteins such as mucin binding protein, surface layer and bacterial hair proteins (Zhang et al., 2023). In a recent study, Liu et al., (2022) demonstrated that *Ilisha elongata* protein significantly enhanced the adhesion capacity of L. plantarum to the jejunum, ileum, cecum and colon epithelium in mice. Similarly, milk immunoglobulins G (ImG) appeared to exhibit a dose-dependent adhesion capacity of B. bifidum to HT-29 cells, which was ascribed to the ability of ImG glycan moieties to modulate the intestinal epithelium cells microstructure for promoting commensals adhesion (Morrin et al., 2020).

In terms of strain specificity, exopolysaccharides (EPS) on the bacterial surface enhance hydrophobicity, thereby increasing the likelihood of adhesion to the mucosal layer (Lu et al., 2022). The production and molecular properties of EPS depend on the available carbon source, which may vary during fermentation (Sørensen et al., 2022). Additionally, bile salt interactions with bacterial surfaces can negatively impact EPS structure (Lu et al., 2022). Interestingly, Martín et al. (2023) reported that increased EPS production in *Lacticaseibacillus rhamnosus* CNCM I-3690 impaired its beneficial effects on the host. These factors may explain the slightly lower number of adhered bacteria when probiotic powders were pre-fermented.

4. Conclusions

This study examined the impact of CPI-fortified probiotic powders on the viability of LGG cells during processing, storage, and static in vitro digestion. CPI effectively incorporated LGG cells into the wall material, with proteomic analysis revealing diverse proteins, including ribosomal proteins, chaperones, and uncharacterized proteins. Digestion increased shorter peptides (\leq 5 amino acids) while reducing longer ones (\geq 12 amino acids), indicating enzymatic proteolysis. Pre-fermentation affected peptide distribution in the food matrix but had no significant impact after digestion. Fermentation compromised LGG resilience during lyophilisation and storage, increasing cell losses, likely due to structural changes and reduced water-binding capacity, but overall viability remained high. The shelf-life of probiotic powders was influenced by storage conditions, with higher temperatures and humidity accelerating bacterial inactivation, while storage at 4 $^{\circ}\text{C}$ and 11 % RH extended shelf-life beyond two years. Simulated gastrointestinal digestion showed significant LGG loss during gastric digestion, with fermentation time influencing resistance to acidity. After intestinal digestion, LGG viability was largely unaffected by intestinal fluids, with fermented powders (CF) showing higher viability than non-fermented powders (CNT), suggesting improved stress-response mechanisms. In the co-culture model, LGG cells adhered well to the mucus-rich epithelium, though pre-fermentation mildly reduced adhesion, potentially due to changes in exopolysaccharide production. The incorporation of CPI into probiotic powders effectively enhanced the stability and functional potential of LGG cells, despite the challenges posed by fermentation and processing conditions, and can thus serve as a promising approach for the development of probiotic powders.

CRediT authorship contribution statement

Jennyfer Fortuin: Writing – review & editing, Writing – original draft, Investigation, Funding acquisition, Formal analysis, Conceptualization. Céline C. Leclercq: Writing – review & editing, Investigation. Rayssa K. Silva: Writing – review & editing, Investigation. Alexander S. Shaplov: Writing – review & editing, Investigation. Sébastien Cambier: Writing – review & editing, Investigation. Marcus Iken: Writing – review & editing. Vincenzo Fogliano: Writing – review & editing, Supervision, Conceptualization. Christos Soukoulis: Writing – review & editing, Supervision, Project administration, Funding acquisition, Conceptualization.

Declaration of competing interest

The authors declare that they have no known competing financial interests or personal relationships that could have appeared to influence the work reported in this paper.

Acknowledgements

The study was co-financed by the Luxembourg National Research Fund – FNR and PM-International AG (Project: ALGPRO, Project number: 15878670, Funding Scheme: Industrial Fellowships).

Appendix A. Supplementary data

Supplementary data to this article can be found online at https://doi.org/10.1016/j.foodhyd.2025.111999.

Data availability

Data will be made available on request.

References

- Ahmed, J., & Kumar, V. (2022). Effect of high-pressure treatment on oscillatory rheology, particle size distribution and microstructure of microalgae Chlorella vulgaris and Arthrospira platensis. Algal Research, 62, Article 102617. https://doi.org/10.1016/j.algal.2021.102617
- Al-Muhtaseb, A. H., McMinn, W. A. M., & Magee, T. R. A. (2002). Moisture sorption isotherm characteristics of food products: A review. Food and Bioproducts Processing, 80(2), 118–128. https://doi.org/10.1205/09603080252938753
- Albalasmeh, A., Berhe, A., & Ghezzehei, T. (2013). A new method for rapid determination of carbohydrate and total carbon concentrations using UV spectrophotometry. Carbohydrate Polymers, 97, 253–261. https://doi.org/10.1016/j. carbpol.2013.04.072
- Aschenbrenner, M., Foerst, P., & Kulozik, U. (2015). Freeze-drying of probiotics. In Advances in Probiotic technol (pp. 213–241). CRC Press. Scopus https://www.scopus.com/inward/record.uri?eid=2-s2.0-85134460327&partnerID=40&md5=a1660f65d781cc9bd94402234d4fabdc.
- Aschenbrenner, M., Kulozik, U., & Foerst, P. (2012). Evaluation of the relevance of the glassy state as stability criterion for freeze-dried bacteria by application of the Arrhenius and WLF model. Cryobiology, 65(3), 308–318. https://doi.org/10.1016/j. cryobiol.2012.08.005
- Becker, E. W. (2007). Micro-algae as a source of protein. Biotechnology Advances, 25(2), 207–210. https://doi.org/10.1016/j.biotechadv.2006.11.002
- Beheshtipour, H., Mortazavian, A. M., Haratian, P., & Darani, K. K. (2012). Effects of Chlorella vulgaris and Arthrospira platensis addition on viability of probiotic bacteria in yogurt and its biochemical properties. European Food Research and Technology, 235 (4), 719–728. https://doi.org/10.1007/s00217-012-1798-4
- Bhutto, R. A., Bhutto, N. ul ain H., Mahar, H., Khanal, S., Wang, M., Iqbal, S., Fan, Y., & Yi, J. (2025). Recent trends in co-encapsulation of probiotics with prebiotics and their applications in the food industry. *Trends in Food Science & Technology*, 156, Article 104829. https://doi.org/10.1016/j.tifs.2024.104829
- Bito, T., Okumura, E., Fujishima, M., & Watanabe, F. (2020). Potential of chlorella as a dietary supplement to promote human health. *Nutrients*, 12(9), 2524. https://doi. org/10.3390/nu12092524
- Brodkorb, A., Egger, L., Alminger, M., Alvito, P., Assunção, R., Ballance, S., Bohn, T., Bourlieu-Lacanal, C., Boutrou, R., Carrière, F., Clemente, A., Corredig, M., Dupont, D., Dufour, C., Edwards, C., Golding, M., Karakaya, S., Kirkhus, B., Le Feunteun, S., ... Recio, I. (2019). INFOGEST static in vitro simulation of gastrointestinal food digestion. Nature Protocols, 14(4), 991–1014. https://doi.org/10.1038/s41596-018-0119-1
- Broeckx, G., Vandenheuvel, D., Henkens, T., Kiekens, S., van den Broek, M. F. L., Lebeer, S., & Kiekens, F. (2017). Enhancing the viability of *Lactobacillus rhamnosus* GG after spray drying and during storage. *International Journal of Pharmaceutics*, 534 (1–2), 35–41. https://doi.org/10.1016/j.ijpharm.2017.09.075. Scopus.
- Burgain, J., Corgneau, M., Scher, J., & Gaiani, C. (2015). Chapter 20—Encapsulation of probiotics in milk protein microcapsules. In L. M. C. Sagis (Ed.), *Microencapsulation* and microspheres for food applications (pp. 391–406). Academic Press. https://doi. org/10.1016/B978-0-12-800350-3.00019-4.
- Cantú-Bernal, S., Domínguez-Gámez, M., Medina-Peraza, I., Aros-Uzarraga, E., Ontiveros, N., Flores-Mendoza, L., Gomez-Flores, R., Tamez-Guerra, P., & González-Ochoa, G. (2020). Enhanced viability and anti-rotavirus effect of Bifidobacterium longum and Lactobacillus plantarum in combination with Chlorella sorokiniana in a dairy product. Frontiers in Microbiology, 11, Article Scopus. https://doi.org/10.3389/fmicb.2020.00875
- Capela, P., Hay, T. K. C., & Shah, N. P. (2006). Effect of cryoprotectants, prebiotics and microencapsulation on survival of probiotic organisms in yoghurt and freeze-dried yoghurt. Food Research International, 39(2), 203–211. https://doi.org/10.1016/j. foodres.2005.07.007. Scopus.

- Capozzi, V., Arena, M. P., Russo, P., Spano, G., & Fiocco, D. (2016). Chapter 16 Stressors and food environment: Toward strategies to improve robustness and stress tolerance in probiotics. In R. R. Watson, & V. R. Preedy (Eds.), *Probiotics, prebiotics, and* synbiotics (pp. 245–256). Academic Press. https://doi.org/10.1016/B978-0-12-802189-7 00016-2
- Chen, K., Ahmad, M. I., Jiang, Q., & Zhang, H. (2024). Acid-induced hydrogels of edible Chlorella pyrenoidosa protein with composite biopolymers network. Food Chemistry, 460, Article 140699. https://doi.org/10.1016/j.foodchem.2024.140699
- Costa, M. M., Spínola, M. P., Alves, V. D., & Mestre Prates, J. A. (2024). Improving protein extraction and peptide production from *Chlorella vulgaris* using combined mechanical/physical and enzymatic pre-treatments. *Heliyon*, 10(12), Article e32704. https://doi.org/10.1016/j.heliyon.2024.e32704
- Cui, S., Hang, F., Liu, X., Xu, Z., Liu, Z., Zhao, J., Zhang, H., & Chen, W. (2018). Effect of acids produced from carbohydrate metabolism in cryoprotectants on the viability of freeze-dried *Lactobacillus* and prediction of optimal initial cell concentration. *Journal* of Bioscience and Bioengineering, 125(5), 513–518. https://doi.org/10.1016/j. jbiosc.2017.12.009. Scopus.
- De Boever, P., Wouters, R., Verschaeve, L., Berckmans, P., Schoeters, G., & Verstraete, W. (2000). Protective effect of the bile salt hydrolase-active *Lactobacillus reuteri* against bile salt cytotoxicity. *Applied Microbiology and Biotechnology*, 53(6), 709–714. https://doi.org/10.1007/s002530000330
- de Deus, C., Duque-Soto, C., Rueda-Robles, A., Martínez-Baena, D., Borrás-Linares, I., Quirantes-Piné, R., Ragagnin de Menezes, C., & Lozano-Sánchez, J. (2024). Stability of probiotics through encapsulation: Comparative analysis of current methods and solutions. Food Research International, 197, Article 115183. https://doi.org/10.1016/ j.foodres.2024.115183
- Dos Santos Morais, R., Gaiani, C., Borges, F., & Burgain, J. (2022). Interactions microbe-matrix in dairy products. In P. L. H. McSweeney, & J. P. McNamara (Eds.), Encyclopedia of dairy sciences (3rd ed., pp. 133–143). Academic Press. https://doi.org/10.1016/B978-0-08-100596-5.23004-7.
- Flach, J., van der Waal, M. B., van den Nieuwboer, M., Claassen, E., & Larsen, O. F. A. (2018). The underexposed role of food matrices in probiotic products: Reviewing the relationship between carrier matrices and product parameters. Critical Reviews in Food Science and Nutrition, 58(15), 2570–2584. https://doi.org/10.1080/10408398.2017.1334624
- Foley, M. H., O'Flaherty, S., Allen, G., Rivera, A. J., Stewart, A. K., Barrangou, R., & Theriot, C. M. (2021). Lactobacillus bile salt hydrolase substrate specificity governs bacterial fitness and host colonization. Proceedings of the National Academy of Sciences, 118(6), Article e2017709118. https://doi.org/10.1073/pnas.2017709118
- Fortuin, J., Hellebois, T., Iken, M., Shaplov, A. S., Fogliano, V., & Soukoulis, C. (2024). Stabilising and functional effects of Spirulina (Arthrospira platensis) protein isolate on encapsulated Lacticaseibacillus rhamnosus GG during processing, storage and gastrointestinal digestion. Food Hydrocolloids, 149, Article 109519. https://doi.org/ 10.1016/j.foodhyd.2023.109519
- Fortuin, J., Leclercq, C. C., Iken, M., Villas-Boas, S. G., & Soukoulis, C. (2025). Proteomic and peptidomic profiling of spirulina-fortified probiotic powder formulations during in vitro digestion. *International Journal of Biological Macromolecules*., Article 140432. https://doi.org/10.1016/j.ijhipmac.2025.140432
- https://doi.org/10.1016/j.ijbiomac.2025.140432

 Garcia-Brand, A. J., Quezada, V., Gonzalez-Melo, C., Bolaños-Barbosa, A. D., Cruz, J. C., & Reyes, L. H. (2022). Novel developments on stimuli-responsive probiotic encapsulates: From smart hydrogels to nanostructured platforms. Fermentation, 8(3), Article Scopus. https://doi.org/10.3390/fermentation8030117
- Gil-Rodríguez, A. M., & Beresford, T. (2021). Bile salt hydrolase and lipase inhibitory activity in reconstituted skim milk fermented with lactic acid bacteria. *Journal of Functional Foods*, 77, Article 104342. https://doi.org/10.1016/j.jff.2020.104342
- Gomand, F., Borges, F., Guerin, J., El-Kirat-Chatel, S., Francius, G., Dumas, D., Burgain, J., & Gaiani, C. (2019). Adhesive interactions between lactic acid bacteria and β-Lactoglobulin: Specificity and impact on bacterial location in whey protein isolate. Frontiers in Microbiology, 10. https://www.frontiersin.org/article/10.33 89/fmicb.2019.01512.
- Grossmann, L., Hinrichs, J., Goff, H. D., & Weiss, J. (2019). Heat-induced gel formation of a protein-rich extract from the microalga Chlorella sorokiniana. Innovative Food Science & Emerging Technologies, 56, Article 102176. https://doi.org/10.1016/j. ifset 2019.06.001
- Grossmann, L., Hinrichs, J., & Weiss, J. (2020). Cultivation and downstream processing of microalgae and Cyanobacteria to generate protein-based technofunctional food ingredients. Critical Reviews in Food Science and Nutrition, 60(17), 17. https://doi. org/10.1080/10408398.2019.1672137
- Gu, Q., Yin, Y., Yan, X., Liu, X., Liu, F., & McClements, D. J. (2022). Encapsulation of multiple probiotics, synbiotics, or nutrabiotics for improved health effects: A review. Advances in Colloid and Interface Science, 309, Article 102781. https://doi.org/ 10.1016/i.cis.2022.102781
- Guarnieri, M. T., Nag, A., Yang, S., & Pienkos, P. T. (2013). Proteomic analysis of Chlorella vulgaris: Potential targets for enhanced lipid accumulation. Journal of Proteomics, 93, 245–253. https://doi.org/10.1016/j.jprot.2013.05.025
- Guerin, J., Burgain, J., Francius, G., El-Kirat-Chatel, S., Beaussart, A., Scher, J., & Gaiani, C. (2018). Adhesion of *Lactobacillus rhamnosus* GG surface biomolecules to milk proteins. *Food Hydrocolloids*, 82, 296–303. https://doi.org/10.1016/j.foodhyd.2018.04.016
- Hadinoto, K., Ling, J. K.-U., Pu, S., & Tran, T.-T. (2024). Effects of alkaline extraction pH on amino acid compositions, protein secondary structures, thermal stability, and functionalities of Brewer's spent grain proteins. *International Journal of Molecular Sciences*, 25(12), 12. https://doi.org/10.3390/ijms25126369
- Hartl, F. U., Bracher, A., & Hayer-Hartl, M. (2011). Molecular chaperones in protein folding and proteostasis. *Nature*, 475(7356), 324–332. https://doi.org/10.1038/ nature10317

- Hellebois, T., Canuel, R., Addiego, F., Audinot, J.-N., Gaiani, C., Shaplov, A. S., & Soukoulis, C. (2023). Milk protein-based cryogel monoliths as novel encapsulants of probiotic bacteria. Part I: Microstructural, physicochemical, and mechanical characterisation. Food Hydrocolloids, 140. https://doi.org/10.1016/j.foodhyd.2023.108641. Scopus.
- Hellebois, T., Canuel, R., Leclercq, C. C., Gaiani, C., & Soukoulis, C. (2024). Milk protein-based cryogel monoliths as novel encapsulants of probiotic bacteria. Part II: Lacticaseibacillus rhamnosus GG storage stability and bioactivity under in vitro digestion. Food Hydrocolloids, 146, Article 109173. https://doi.org/10.1016/j.foodhyd.2023.109173
- Hellebois, T., Fortuin, J., Cambier, S., Contal, S., Leclercq, C. C., Gaiani, C., & Soukoulis, C. (2024). Stability and adhesion properties of *Lacticaseibacillus rhamnosus* GG embedded in milk protein cryogels: Influence of plant seed gum inclusion. *Food Hydrocolloids*, 151, Article 109867. https://doi.org/10.1016/j.foodhyd.2024.109867
- Henchion, M., Hayes, M., Mullen, A. M., Fenelon, M., & Tiwari, B. (2017). Future protein supply and demand: Strategies and factors influencing a sustainable equilibrium. *Foods*, 6(7), 7. https://doi.org/10.3390/foods6070053
- Hernández-Gómez, J. G., López-Bonilla, A., Trejo-Tapia, G., Ávila-Reyes, S. V., Jiménez-Aparicio, A. R., & Hernández-Sánchez, H. (2021). In vitro Bile Salt Hydrolase (BSH) activity screening of different probiotic microorganisms. Foods, 10(3), 674. https://doi.org/10.3390/foods10030674
- Hlaing, M. M., Wood, B. R., McNaughton, D., Ying, D., Dumsday, G., & Augustin, M. A. (2017). Effect of drying methods on protein and DNA conformation changes in Lactobacillus rhamnosus GG cells by fourier transform infrared spectroscopy. Journal of Agricultural and Food Chemistry, 65(8), 1724–1731. https://doi.org/10.1021/acs.jafc.6b05508. Scopus.
- Hoobin, P., Burgar, I., Zhu, S., Ying, D., Sanguansri, L., & Augustin, M. A. (2013). Water sorption properties, molecular mobility and probiotic survival in freeze dried protein-carbohydrate matrices. Food & Function, 4(9), 1376–1386. https://doi.org/10.1039/c3fo60112a. Scopus.
- Huang, H., Lang, Y., & Zhou, M. (2024). A comprehensive review on medical applications of microalgae. *Algal Research*, 80, Article 103504. https://doi.org/10.1016/j. algal.2024.103504
- Jackson, M., & Mantsch, H. H. (1995). The use and misuse of FTIR spectroscopy in the determination of protein structure. Critical Reviews in Biochemistry and Molecular Biology, 30(2), 95–120. https://doi.org/10.3109/10409239509085140
- Kieliszek, M., Pobiega, K., Piwowarek, K., & Kot, A. M. (2021). Characteristics of the proteolytic enzymes produced by lactic acid bacteria. *Molecules*, 26(7), 1858. https://doi.org/10.3390/molecules26071858
- Kiepś, J., & Dembczyński, R. (2022). Current trends in the production of probiotic formulations. *Foods*, 11(15), Article Scopus. https://doi.org/10.3390/ foods11152330
- Kim, W., Wang, Y., Vongsvivut, J., Ye, Q., & Selomulya, C. (2023). On surface composition and stability of β-carotene microcapsules comprising pea/whey protein complexes by synchrotron-FTIR microspectroscopy. *Food Chemistry*, 426, Article Scopus. https://doi.org/10.1016/j.foodchem.2023.136565
- Koskenniemi, K., Laakso, K., Koponen, J., Kankainen, M., Greco, D., Auvinen, P., Savijoki, K., Nyman, T. A., Surakka, A., Salusjärvi, T., de Vos, W. M., Tynkkynen, S., Kalkkinen, N., & Varmanen, P. (2011). Proteomics and transcriptomics characterization of bile stress response in probiotic *Lactobacillus rhamnosus* GG. *Molecular & Cellular Proteomics*, 10(2), S1–S18. https://doi.org/10.1074/mcp. M110.002741
- Ladjal-Ettoumi, Y., Douik, L. H., Hamadi, M., Abdullah, J. A. A., Cherifi, Z., Keddar, M. N., Zidour, M., & Nazir, A. (2024). Physicochemical and functional properties of spirulina and chlorella proteins obtained by iso-electric precipitation. Food Biophysics, 19(2), 439–452. https://doi.org/10.1007/s11483-024-09836-8
 Li, Y., Aiello, G., Fassi, E. M. A., Boschin, G., Bartolomei, M., Bollati, C., Roda, G.,
- Li, Y., Aiello, G., Fassi, E. M. A., Boschin, G., Bartolomei, M., Bollati, C., Roda, G., Arnoldi, A., Grazioso, G., & Lammi, C. (2021). Investigation of *Chlorella pyrenoidosa* protein as a source of novel Angiotensin I-Converting Enzyme (ACE) and Dipeptidyl Peptidase-IV (DPP-IV) inhibitory peptides. *Nutrients*, 13(5), 5. https://doi.org/ 10.3390/mu13051624
- Loveday, S. M. (2022). Protein digestion and absorption: The influence of food processing. *Nutrition Research Reviews*, 1–16. https://doi.org/10.1017/ S0954422422000245
- Lowell, S., & Shields, J. E. (1984). Adsorption isotherms. In S. Lowell, & J. E. Shields (Eds.), Powder surface area and porosity (pp. 11–13). Netherlands: Springer. https://doi.org/10.1007/978-94-009-5562-2 3.
- Lu, Y., Han, S., Zhang, S., Wang, K., Lv, L., McClements, D. J., Xiao, H., Berglund, B., Yao, M., & Li, L. (2022). The role of probiotic exopolysaccharides in adhesion to mucin in different gastrointestinal conditions. Current Research in Food Science, 5, 581–589. https://doi.org/10.1016/j.crfs.2022.02.015
- Madsen, M., Rønne, M. E., Li, R., Greco, I., Ipsen, R., & Svensson, B. (2022). Simulated gastrointestinal digestion of protein alginate complexes: Effects of whey protein cross-linking and the composition and degradation of alginate. Food & Function, 13 (16), 8375–8387. https://doi.org/10.1039/D2F001256A
- Mafe, A. N., Edo, G. I., Majeed, O. S., Gaaz, T. S., Akpoghelie, P. O., Isoje, E. F., Igbuku, U. A., Owheruo, J. O., Opiti, R. A., Garba, Y., Essaghah, A. E. A., Ahmed, D. S., & Umar, H. (2025). A review on probiotics and dietary bioactives: Insights on metabolic well-being, gut microbiota, and inflammatory responses. Food Chemistry Advances, 6, Article 100919. https://doi.org/10.1016/j. focha.2025.100919
- Maftei, N.-M., Raileanu, C. R., Balta, A. A., Ambrose, L., Boev, M., Marin, D. B., & Lisa, E. L. (2024). The potential impact of probiotics on human health: An update on their health-promoting properties. *Microorganisms*, 12(2), 2. https://doi.org/10.3390/microorganisms12020234

- Martín, R., Benítez-Cabello, A., Kulakauskas, S., Viana, M. V. C., Chamignon, C., Courtin, P., Carbonne, C., Chain, F., Pham, H. P., Derrien, M., Bermúdez-Humarán, L. G., Chapot-Chartier, M. P., Smokvina, T., & Langella, P. (2023). Over-production of exopolysaccharide by *Lacticaseibacillus rhamnosus* CNCM I-3690 strain cutbacks its beneficial effect on the host. *Scientific Reports*, 13(1), 6114. https://doi.org/10.1038/s41598-023-32116-3
- Meireles Mafaldo, Í., de Medeiros, V. P. B., da Costa, W. K. A., da Costa Sassi, C. F., da Costa Lima, M., de Souza, E. L., Eduardo Barão, C., Colombo Pimentel, T., & Magnani, M. (2022). Survival during long-term storage, membrane integrity, and ultrastructural aspects of Lactobacillus acidophilus 05 and Lacticaseibacillus casei 01 freeze-dried with freshwater microalgae biomasses. Food Research International, 159, Article 111620. https://doi.org/10.1016/j.foodres.2022.111620
- Mendonça, A. A., Pinto-Neto, W., de, P., da Paixão, G. A., Santos, D. da S., De Morais, M. A., & De Souza, R. B. (2022). Journey of the probiotic bacteria: Survival of the fittest. *Microorganisms*, 11(1), 95. https://doi.org/10.3390/microorganisms.11(10)005
- Metsalu, T., & Vilo, J. (2015). ClustVis: A web tool for visualizing clustering of multivariate data using principal component analysis and heatmap. *Nucleic Acids Research*, 43(W1), W566–W570. https://doi.org/10.1093/nar/gkv468
- Morrin, S. T., McCarthy, G., Kennedy, D., Marotta, M., Irwin, J. A., & Hickey, R. M. (2020). Immunoglobulin G from bovine milk primes intestinal epithelial cells for increased colonization of bifidobacteria. AMB Express, 10, 114. https://doi.org/10.1186/s13568-020-01048-w
- Morris, H. J., Almarales, A., Carrillo, O., & Bermúdez, R. C. (2008). Utilisation of Chlorella vulgaris cell biomass for the production of enzymatic protein hydrolysates. Bioresource Technology, 99(16), 7723–7729. https://doi.org/10.1016/j. biortech.2008.01.080
- Mosibo, O. K., Ferrentino, G., & Udenigwe, C. C. (2024). Microalgae proteins as sustainable ingredients in novel foods: Recent developments and challenges. *Foods*, 13(5), 5. https://doi.org/10.3390/foods13050733
- Mulet-Cabero, A.-I., Mackie, A. R., Wilde, P. J., Fenelon, M. A., & Brodkorb, A. (2019). Structural mechanism and kinetics of in vitro gastric digestion are affected by process-induced changes in bovine milk. Food Hydrocolloids, 86, 172–183. https://doi.org/10.1016/j.foodhyd.2018.03.035
- Nielsen, S. D., Beverly, R. L., Qu, Y., & Dallas, D. C. (2017). Milk bioactive peptide database: A comprehensive database of milk protein-derived bioactive peptides and novel visualization. Food Chemistry, 232, 673–682. https://doi.org/10.1016/j. foodchem.2017.04.056
- Nielsen, S. D.-H., Liang, N., Rathish, H., Kim, B. J., Lueangsakulthai, J., Koh, J., Qu, Y., Schulz, H.-J., & Dallas, D. C. (2023). Bioactive milk peptides: An updated comprehensive overview and database. *Critical Reviews in Food Science and Nutrition*, 1–20. https://doi.org/10.1080/10408398.2023.2240396. 0(0).
- Passot, S., Cenard, S., Douania, I., Tréléa, I. C., & Fonseca, F. (2012). Critical water activity and amorphous state for optimal preservation of lyophilised lactic acid bacteria. Food Chemistry, 132(4), 1699–1705. https://doi.org/10.1016/j. foodchem.2011.06.012
- Paterson, S., Majchrzak, M., Alexandru, D., Di Bella, S., Fernández-Tomé, S., Arranz, E., de la Fuente, M. A., Gómez-Cortés, P., & Hernández-Ledesma, B. (2024). Impact of the biomass pretreatment and simulated gastrointestinal digestion on the digestibility and antioxidant activity of microalgae Chlorella vulgaris and Tetraselmis chuii. Food Chemistry, 453, Article 139686. https://doi.org/10.1016/j.foodchem.2024.139686
- Pehkonen, K. S., Roos, Y. H., Miao, S., Ross, R. P., & Stanton, C. (2008). State transitions and physicochemical aspects of cryoprotection and stabilization in freeze-drying of *Lactobacillus rhamnosus* GG (LGG). *Journal of Applied Microbiology*, 104(6), 1732–1743. https://doi.org/10.1111/j.1365-2672.2007.03719.x. Scopus.
- Qadri, H., Shah, A. H., Almilaibary, A., & Mir, M. A. (2024). Microbiota, natural products, and human health: Exploring interactions for therapeutic insights. Frontiers in Cellular and Infection Microbiology, 14. https://doi.org/10.3389/ fcimb.2024.1371312
- Ruiz, L., Margolles, A., & Sánchez, B. (2013). Bile resistance mechanisms in *Lactobacillus* and *Bifidobacterium*. Frontiers in Microbiology, 4, 396. https://doi.org/10.3389/fmicb.2013.00396
- Safi, C., Charton, M., Pignolet, O., Pontalier, P.-Y., & Vaca-Garcia, C. (2013). Evaluation of the protein quality of Porphyridium cruentum. Journal of Applied Phycology, 25(2), 497–501. https://doi.org/10.1007/s10811-012-9883-4
- Safi, C., Charton, M., Pignolet, O., Silvestre, F., Vaca-Garcia, C., & Pontalier, P.-Y. (2013). Influence of microalgae cell wall characteristics on protein extractability and determination of nitrogen-to-protein conversion factors. *Journal of Applied Phycology*, 25(2), 523–529. https://doi.org/10.1007/s10811-012-9886-1
- Safi, C., Zebib, B., Merah, O., Pontalier, P.-Y., & Vaca-Garcia, C. (2014). Morphology, composition, production, processing and applications of *Chlorella vulgaris*: A review. Renewable and Sustainable Energy Reviews, 35, 265–278. https://doi.org/10.1016/j.rser.2014.04.007
- Schwab, C., Vogel, R., & Gänzle, M. G. (2007). Influence of oligosaccharides on the viability and membrane properties of *Lactobacillus reuteri* TMW1.106 during freezedrying. *Cryobiology*, 55(2), 108–114. https://doi.org/10.1016/j. cryobiol.2007.06.004
- Seifert, A., Kashi, Y., & Livney, Y. D. (2019). Delivery to the gut microbiota: A rapidly proliferating research field. Advances in Colloid and Interface Science, 274, Article 102038. https://doi.org/10.1016/j.cis.2019.102038
- Sørensen, H. M., Rochfort, K. D., Maye, S., MacLeod, G., Brabazon, D., Loscher, C., & Freeland, B. (2022). Exopolysaccharides of lactic acid bacteria: Production, purification and health benefits towards functional food. *Nutrients*, 14(14), 2938. https://doi.org/10.3390/nu14142938

- Soukoulis, C., Behboudi-Jobbehdar, S., Yonekura, L., Parmenter, C., & Fisk, I. (2014). Impact of milk protein type on the viability and storage stability of microencapsulated *Lactobacillus acidophilus* NCIMB 701748 using spray drying. *Food and Bioprocess Technology*, 7(5), 1255–1268. https://doi.org/10.1007/s11947-013-1120-x
- Soukoulis, C., Yonekura, L., Gan, H.-H., Behboudi-Jobbehdar, S., Parmenter, C., & Fisk, I. (2014). Probiotic edible films as a new strategy for developing functional bakery products: The case of pan bread. Food Hydrocolloids, 39, 231–242. https://doi.org/10.1016/j.foodhyd.2014.01.023
- Świątecka, D., Małgorzata, I., Aleksander, Ś., Henryk, K., & Elżbieta, K. (2010). The impact of glycated pea proteins on bacterial adhesion. Food Research International, 43 (6), 1566–1576. https://doi.org/10.1016/j.foodres.2010.03.003
- Talebian, S., Schofield, T., Valtchev, P., Schindeler, A., Kavanagh, J. M., Adil, Q., & Dehghani, F. (2022). Biopolymer-based multilayer microparticles for probiotic delivery to Colon. Advanced Healthcare Materials, 11(11), Article 2102487. https://doi.org/10.1002/adhm.202102487
- Tallon, R., Arias, S., Bressollier, P., & Urdaci, M. C. (2007). Strain- and matrix-dependent adhesion of *Lactobacillus plantarum* is mediated by proteinaceous bacterial compounds. *Journal of Applied Microbiology*, 102(2), 442–451. https://doi.org/ 10.1111/j.1365-2672.2006.03086.x
- Ursu, A.-V., Marcati, A., Sayd, T., Sante-Lhoutellier, V., Djelveh, G., & Michaud, P. (2014). Extraction, fractionation and functional properties of proteins from the microalgae Chlorella vulgaris. Bioresource Technology, 157, 134–139. https://doi.org/10.1016/j.biortech.2014.01.071
- van Boekel, M. A. J. S. (2002). On the use of the Weibull model to describe thermal inactivation of microbial vegetative cells. *International Journal of Food Microbiology*, 74(1), 139–159. https://doi.org/10.1016/S0168-1605(01)00742-5

- van Boekel, M. A. J. S. (2009). Kinetic modeling of reactions in foods. CRC Press.
- van den Berg, C., & Bruin, S. (1981). Water activity and its estimation in food systems: Theoretical aspects. In Water activity: Influences on food quality (pp. 1–61). Elsevier. https://doi.org/10.1016/B978-0-12-591350-8.50007-3.
- Wang, D., Xu, R., Liu, S., Sun, X., Zhang, T., Shi, L., & Wang, Y. (2025). Enhancing the application of probiotics in probiotic food products from the perspective of improving stress resistance by regulating cell physiological function: A review. Food Research International, 199, Article 115369. https://doi.org/10.1016/j.foodres.2024.115369
- Wilson, D. N., & Cate, J. H. D. (2012). The structure and function of the eukaryotic ribosome. Cold Spring Harbor Perspectives in Biology, 4(5), Article a011536. https://doi.org/10.1101/cshperspect.a011536
- Xiao, Z., Han, Q., Chen, K., Yang, J., Yang, H., Zhang, Y., & Wu, L. (2024). The impact of extraction processes on the physicochemical, functional properties and structures of bamboo shoot protein. Food Research International, 187, Article 114368. https://doi. org/10.1016/j.foodres.2024.114368
- Yao, M., Xie, J., Du, H., McClements, D. J., Xiao, H., & Li, L. (2020). Progress in microencapsulation of probiotics: A review. Comprehensive Reviews in Food Science and Food Safety, 19(2), 857–874. https://doi.org/10.1111/1541-4337.12532
- Ying, D. Y., Phoon, M. C., Sanguansri, L., Weerakkody, R., Burgar, I., & Augustin, M. A. (2010). Microencapsulated *Lactobacillus rhamnosus* GG powders: Relationship of powder physical properties to probiotic survival during storage. *Journal of Food Science*, 75(9), E588–E595. https://doi.org/10.1111/j.1750-3841.2010.01838.x
- Ying, D., Sun, J., Sanguansri, L., Weerakkody, R., & Augustin, M. A. (2012). Enhanced survival of spray-dried microencapsulated *Lactobacillus rhamnosus* GG in the presence of glucose. *Journal of Food Engineering*, 109(3), 597–602. https://doi.org/ 10.1016/j.jfoodeng.2011.10.017